Line Profile Variability in AGNs

Wolfram Kollatschny, Göttingen

Serbia, 2007

University Observatory

Institute for Astrophysics

Scale Sizes of an AGN

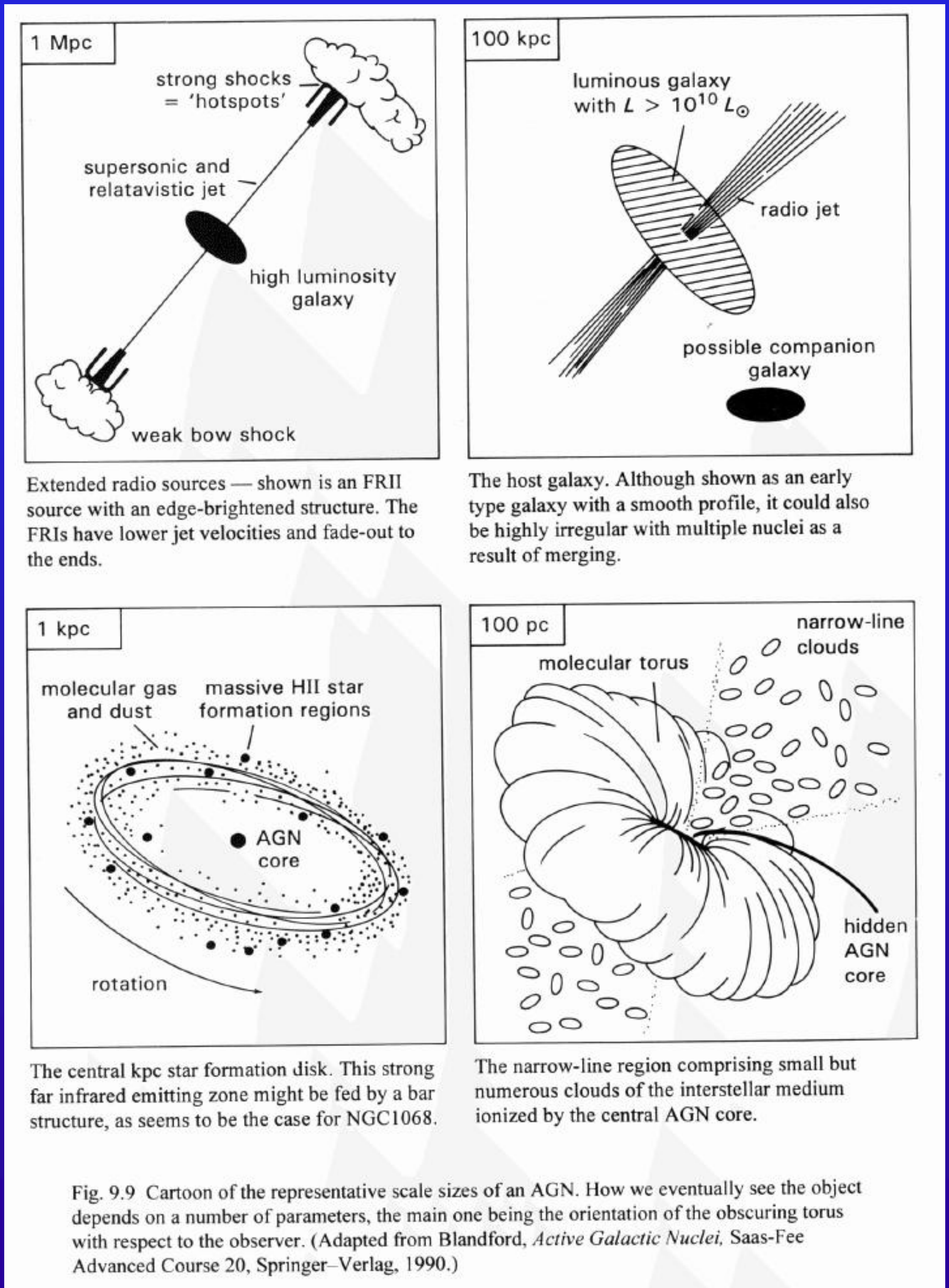

Extended radio sources — shown is an FRII source with an edge-brightened structure. The FRIs have lower jet velocities and fade-out to the ends.

The host galaxy. Although shown as an early type galaxy with a smooth profile, it could also be highly irregular with multiple nuclei as a result of merging.

The central kpc star formation disk. This strong far infrared emitting zone might be fed by a bar structure, as seems to be the case for NGC1068.

The narrow-line region comprising small but numerous clouds of the interstellar medium ionized by the central AGN core.

Fig. 9.9 Cartoon of the representative scale sizes of an AGN. How we eventually see the object depends on a number of parameters, the main one being the orientation of the obscuring torus with respect to the observer. (Adapted from Blandford, *Active Galactic Nuclei,* Saas-Fee Advanced Course 20, Springer–Verlag, 1990.)

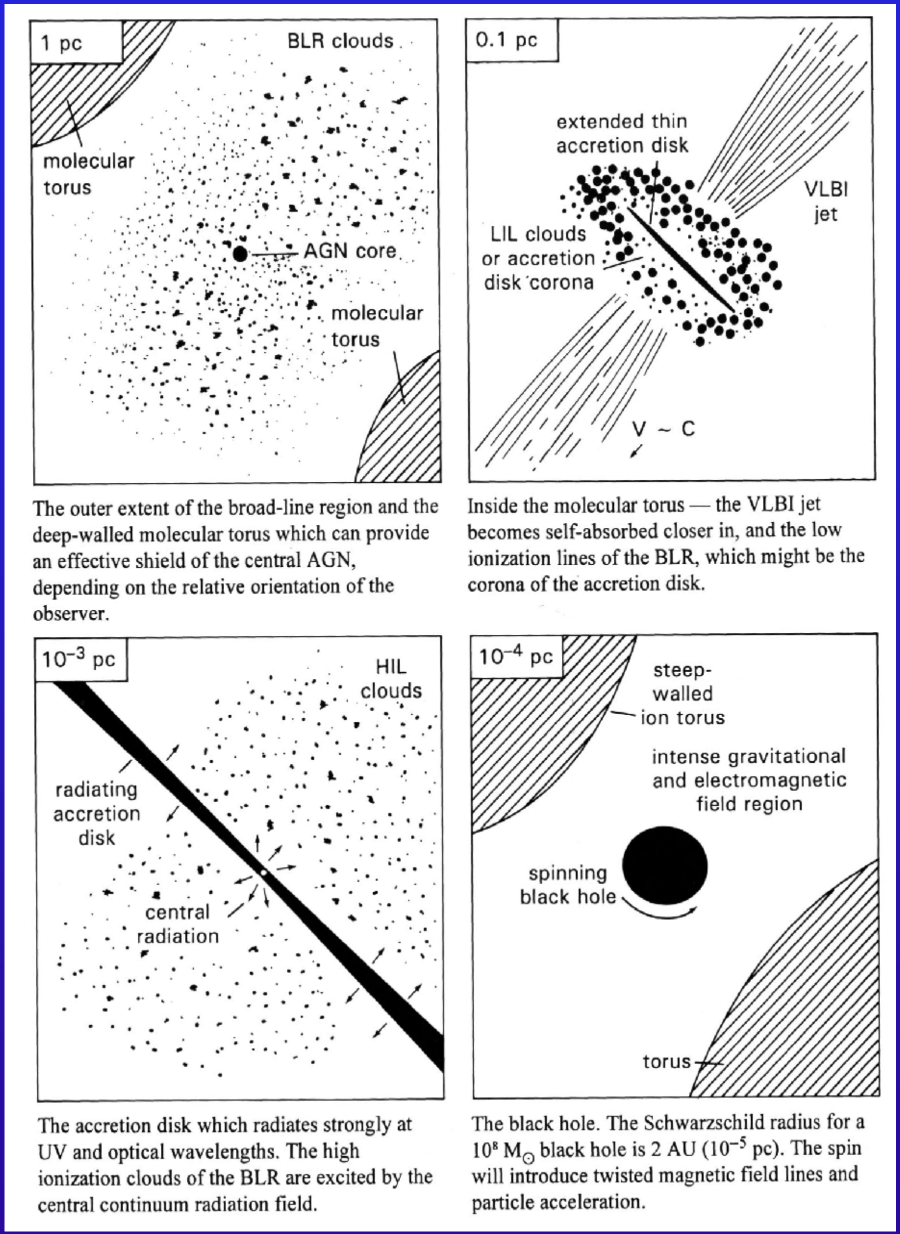

The outer extent of the broad-line region and the deep-walled molecular torus which can provide an effective shield of the central AGN, depending on the relative orientation of the observer.

Inside the molecular torus — the VLBI jet becomes self-absorbed closer in, and the low ionization lines of the BLR, which might be the corona of the accretion disk.

The accretion disk which radiates strongly at UV and optical wavelengths. The high ionization clouds of the BLR are excited by the central continuum radiation field.

The black hole. The Schwarzschild radius for a $10^8 M_\odot$ black hole is 2 AU (10^{-5} pc). The spin will introduce twisted magnetic field lines and particle acceleration.

HST : 0.1“ ≅ 2pc

R. Blandford

1pc = 3.3 ly = 1190. ld = $3 \cdot 10^{18}$ cm

Broad Line Region Structure?

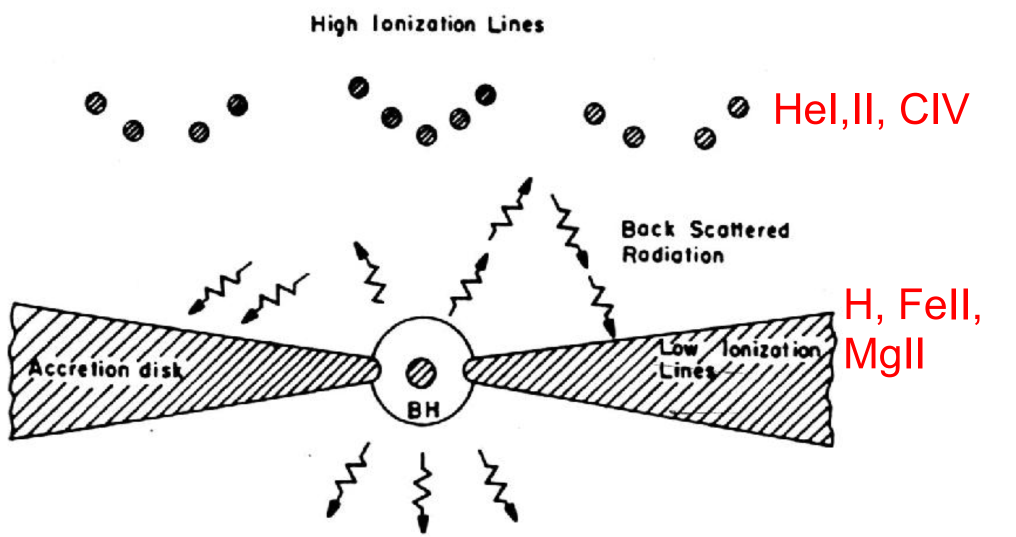

Fig. 13. A schematic two-component model for the BLR. The high ionization lines are emitted in a spherical system of clouds, and are excited by the direct ultraviolet radiation of the central source. The low ionization lines come mainly from the outer regions of the central disk, where most of the line excitation is due to back-scattered, hard ionizing photons. (After Collin-Souffrin, Perry and Dyson(1987), Collin-Souffrin (1987) and Dumont and Collin-Souffrin (1990))

464 EMMERING, BLANDFORD, & SHLOSMAN Vol. 385

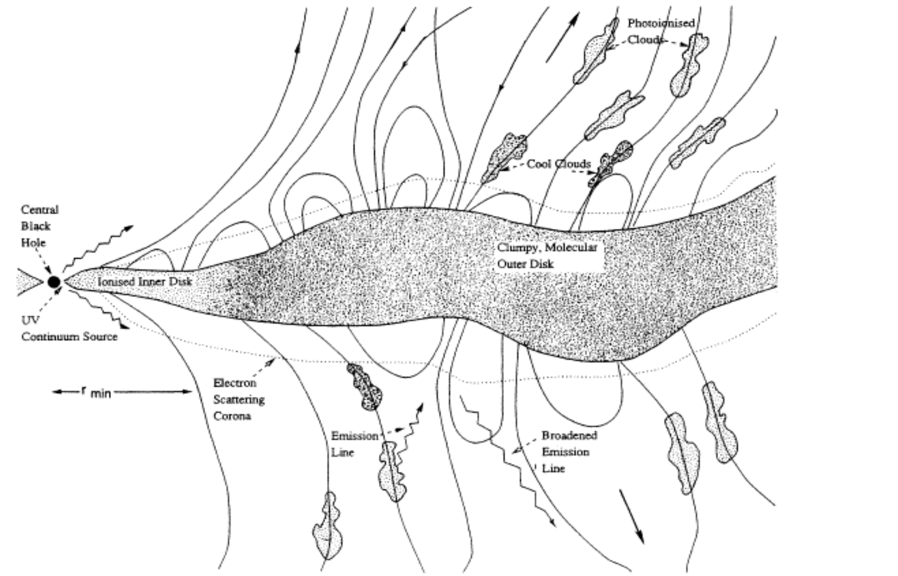

FIG. 1.—Schematic representation of magnetic accretion disk model for broad emission-line region. The accretion disk is ionized in the inner parts but neutral and probably molecular at large radius. Small dense clouds of molecular gas can be radiatively accelerated away from the surface of the disk and flung centrifugally outward along the magnetic field to attain speeds several times the initial Keplerian velocities. When these clouds are exposed to the full UV photoionizing flux, they are heated to temperatures $T \sim 10^4$ K and produce the emission lines. It is possible that these line photons are subsequently scattered by $\sim 10^6$ K electrons, either within a corona or at the disk.

Two component BLR?

Collin-Souffrin et al., 1990

Radiatively accelerated clouds in hydromagnetic wind?

Emmering, Blandford, Shlosman,1992

AGN working model

NGC 3783

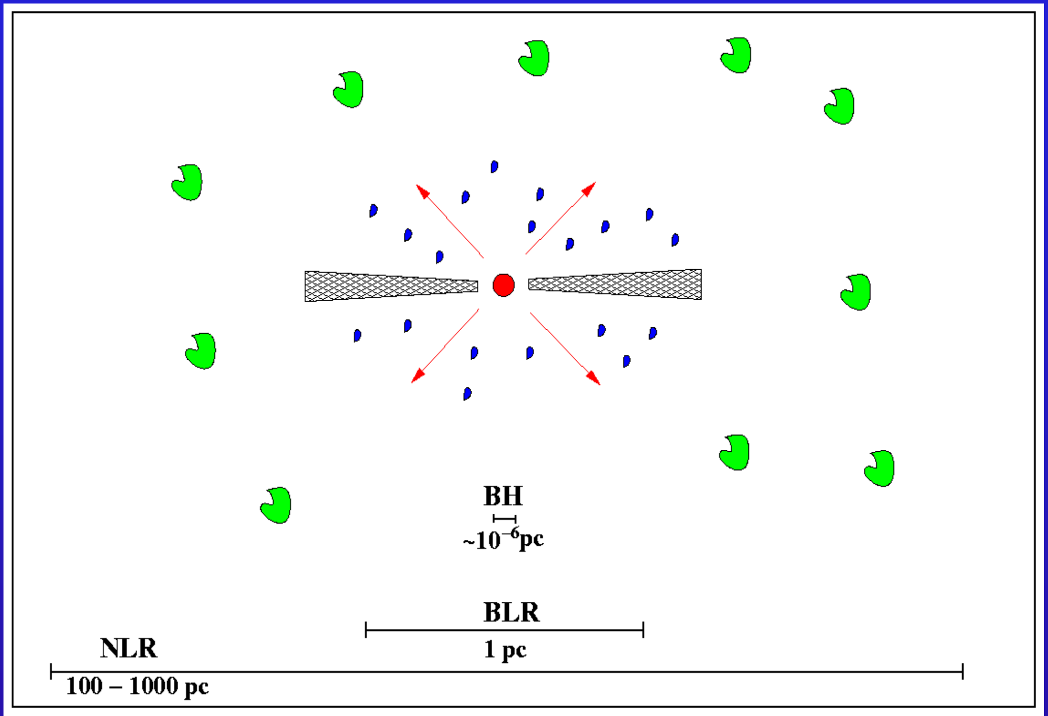

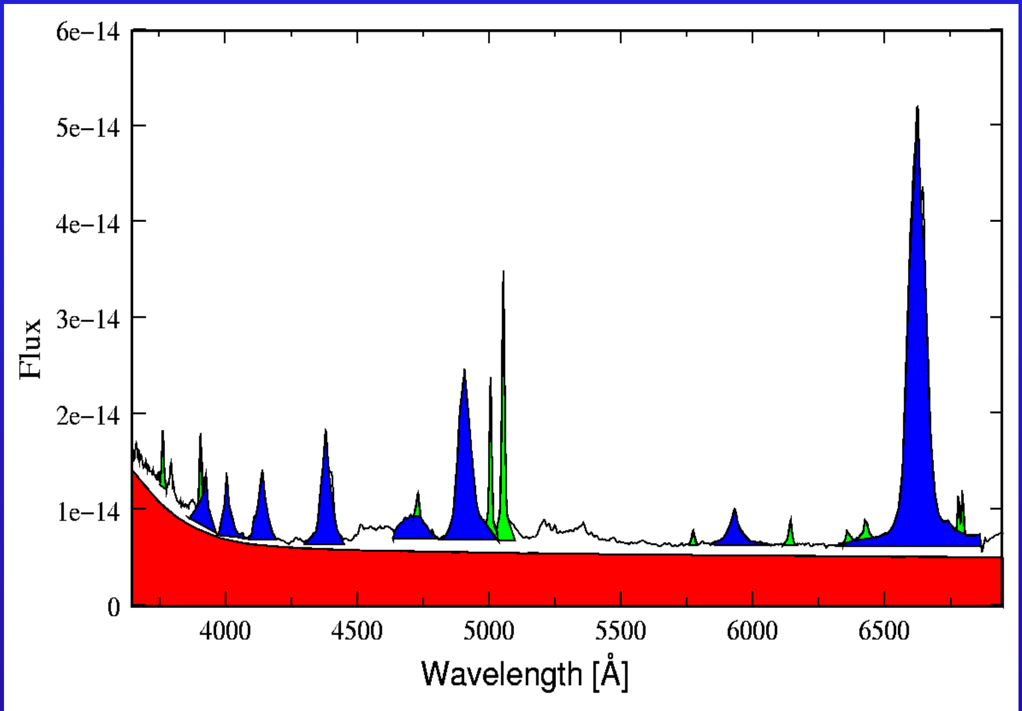

SMBH~10^8 M_O ~ 10^{13}cm

Broad Line Region (<1pc)

Narrow Line Region (~100-1000pc)

geometry, kinematics?

Study of Variability:

-Extension, Structure
-Geometry
-and Kinematics of the central
Broad Line Region in AGN

- Black Hole Mass

in NGC5548, Mrk926, Mrk110

HST Image of NGC5548

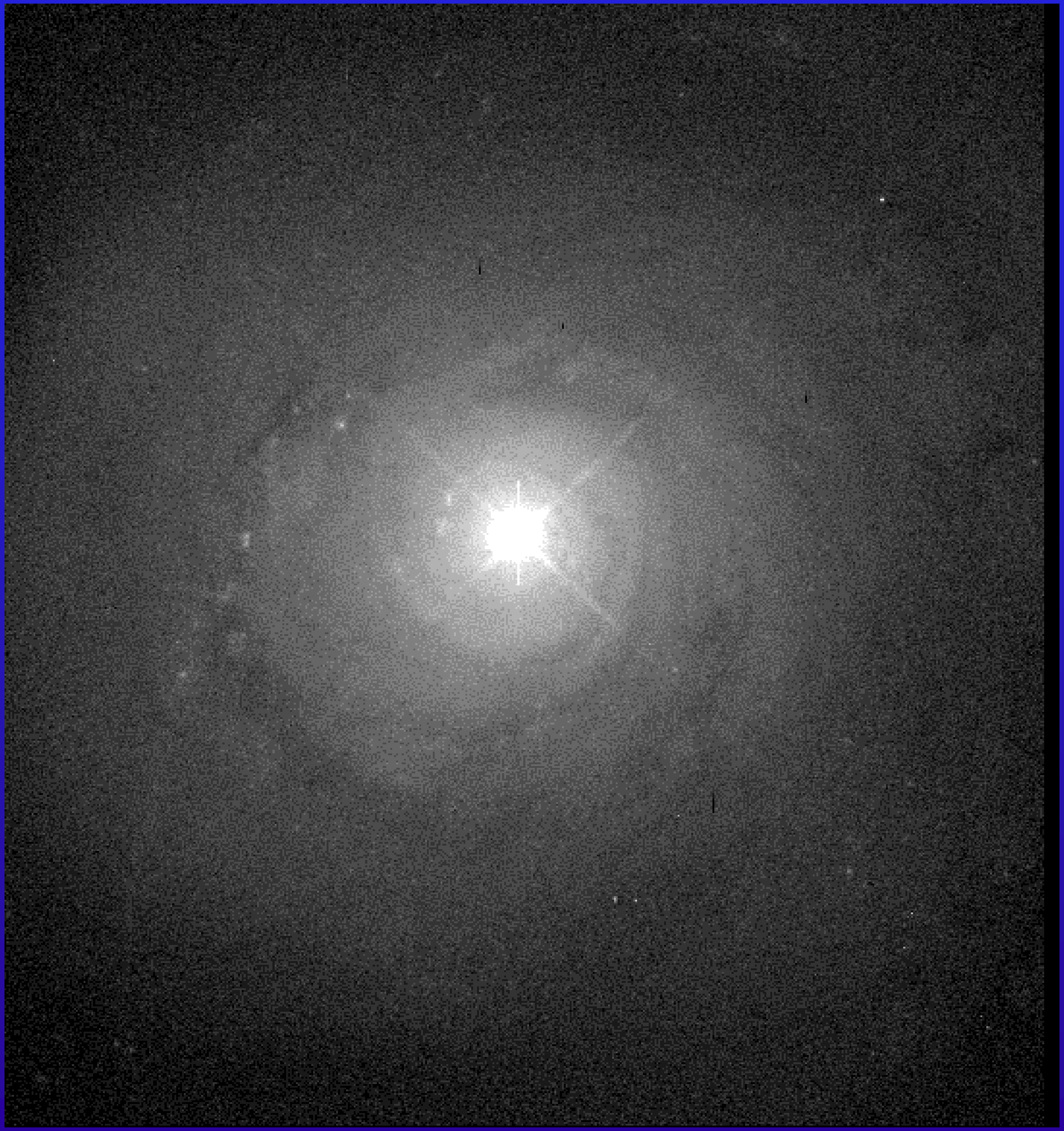

NGC5548

V = 13.7
M_V= -20.7
z = 0.017
FWHM(Hβ)=4400 km s^{-1}

25 x 30 arcsec

High and low state spectra of NGC5548

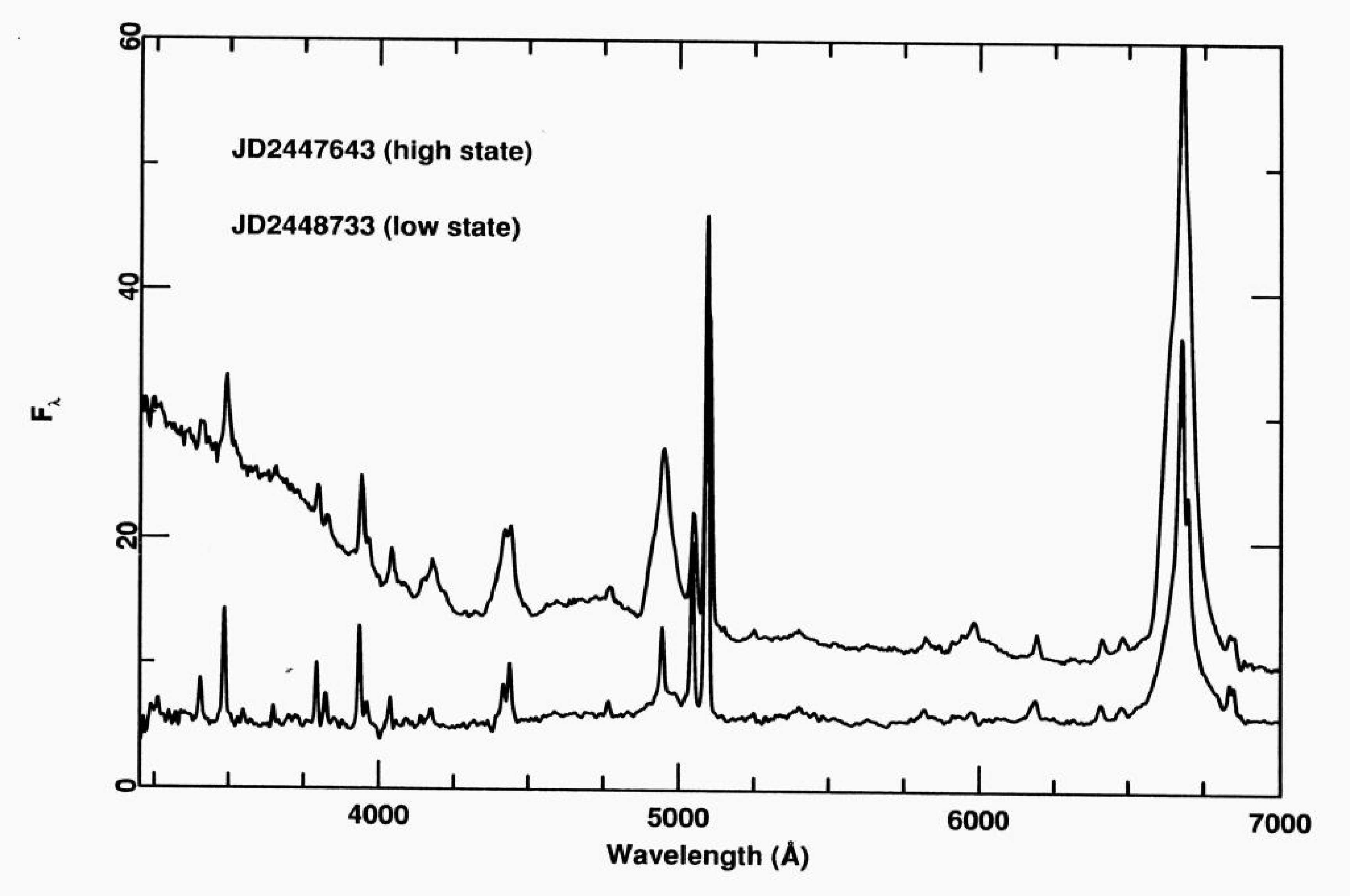

1989

1993

BLR: Idealized Model

Response of BLR clouds on continuum flashes

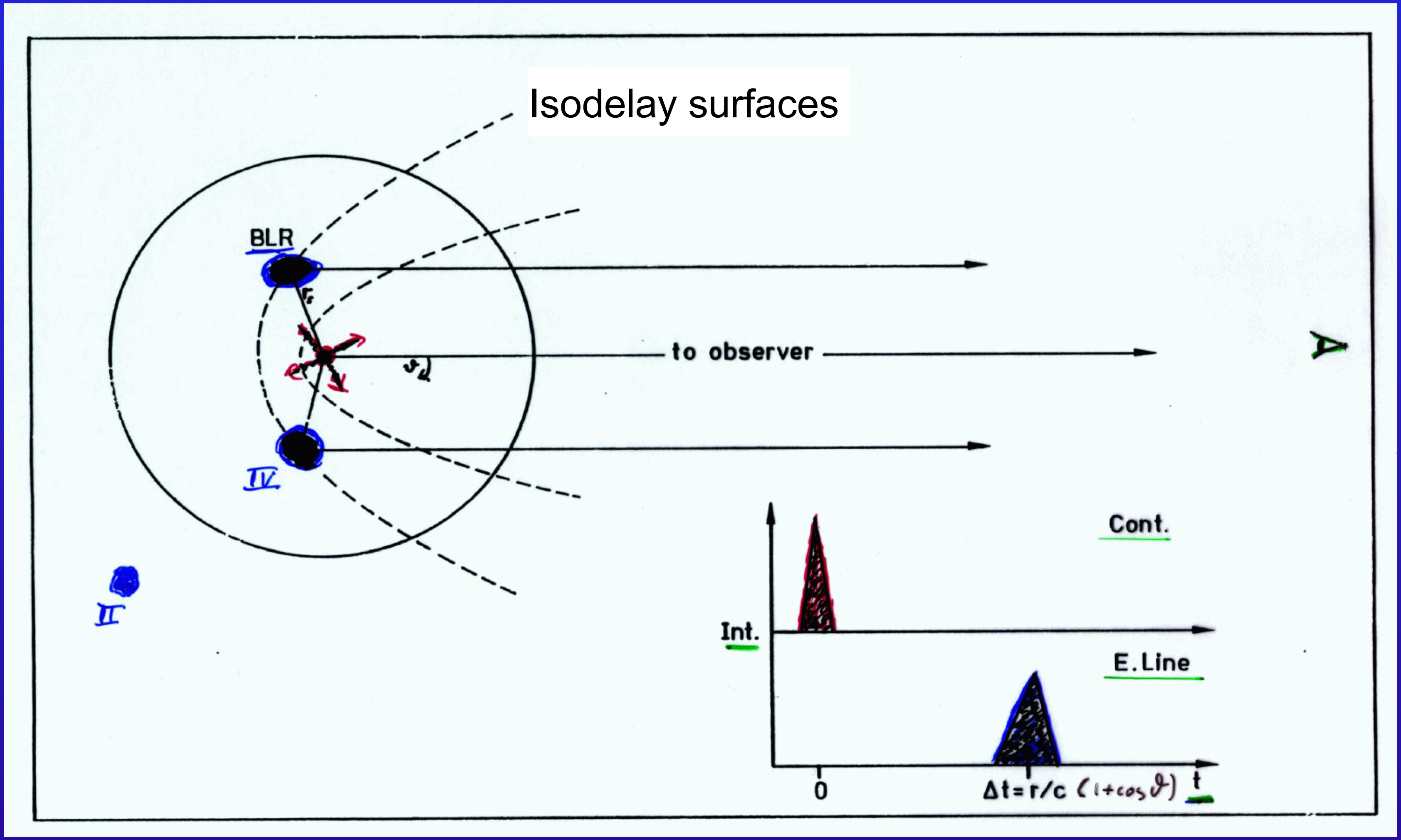

BLR stratification

Delay by light travel time effects

BLR: Continuum & integ. Hβ line variability

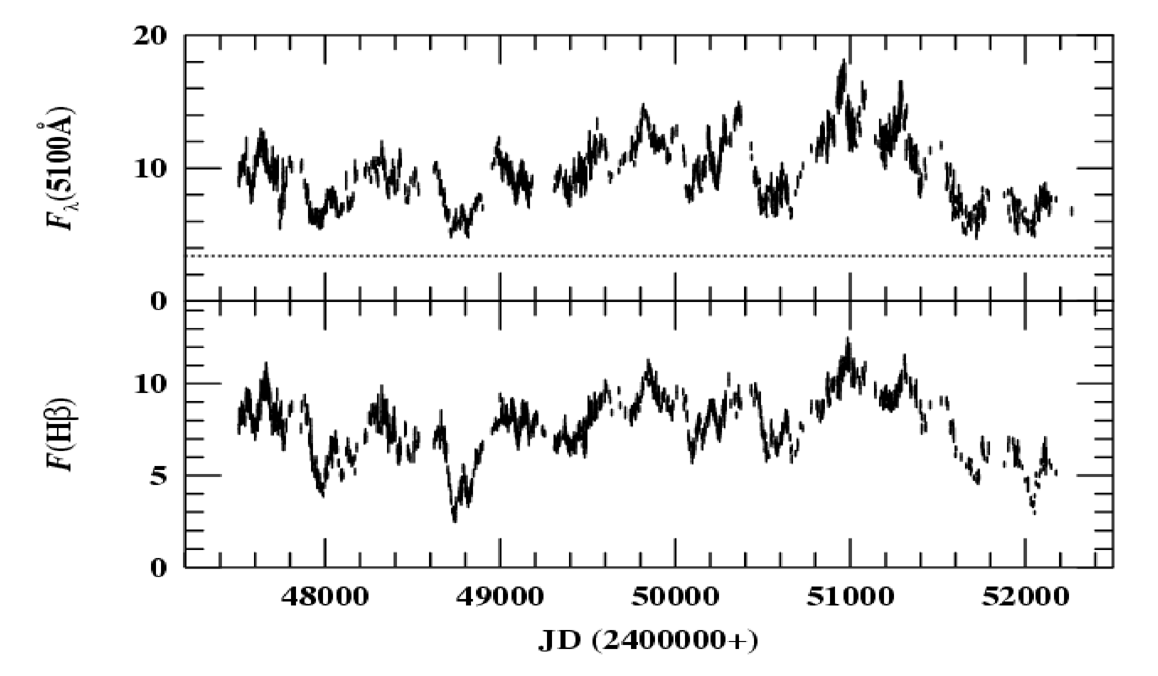

1989 - 2001

NGC 5548

B. Peterson et al., 2002

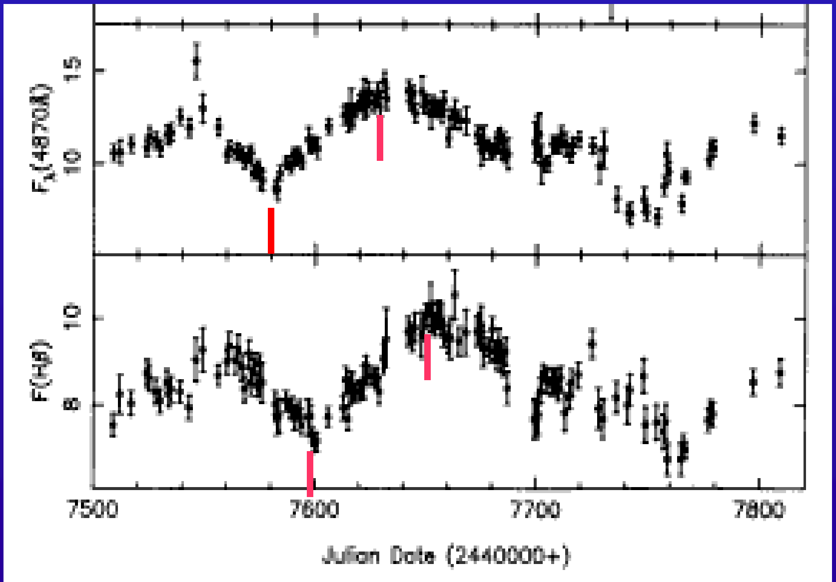

Hβ delay ~ 20 light days

1989

BLR size and stratification in NGC5548

peak to peak
var. ampl.

lightcurves (1989)

ACF, CCF

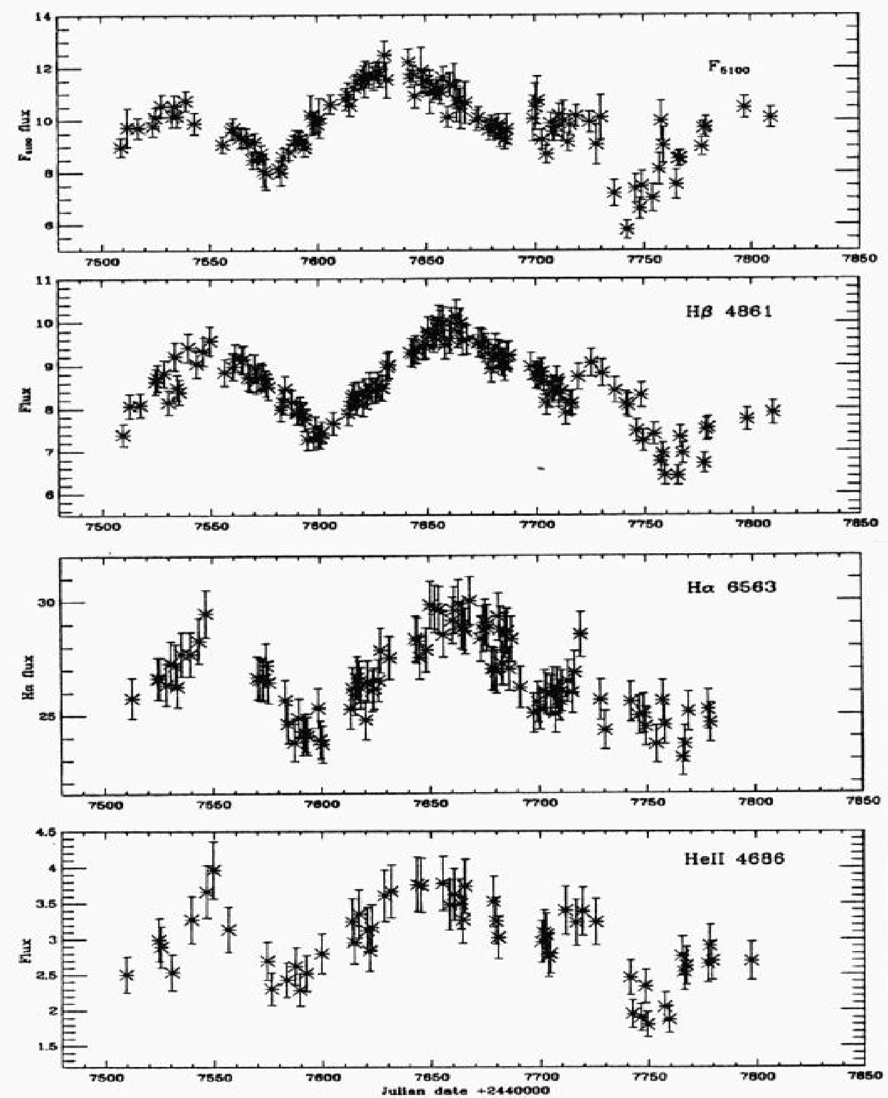

delay

	peak to peak var. ampl.	delay
opt. Cont.	0.56	
Hβ	0.29	19.
Hα	(0.17)	(18.)
HeII	0.61	7.

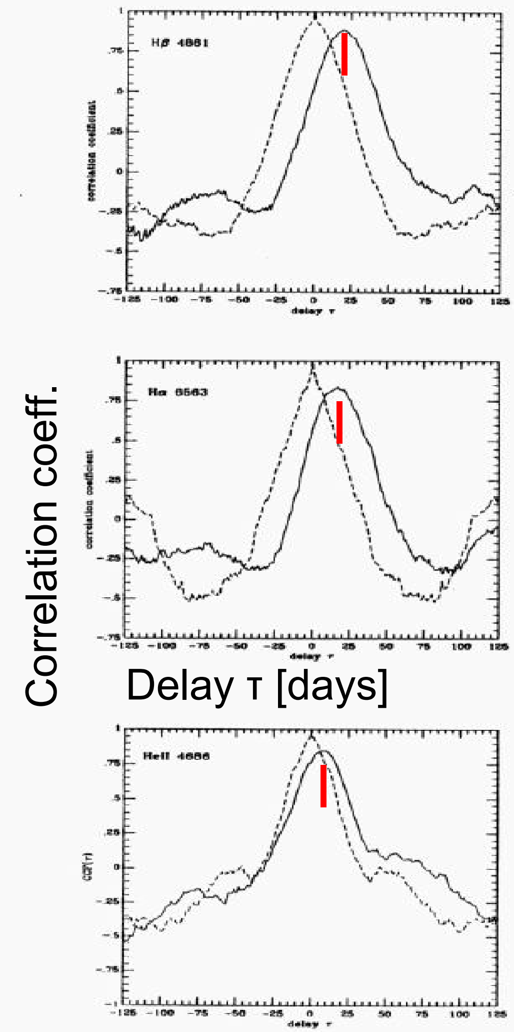

Dietrich, Kollatschny et al., 1994

BLR size and stratification in NGC5548

higher ionized lines: - broader line widths

- faster response

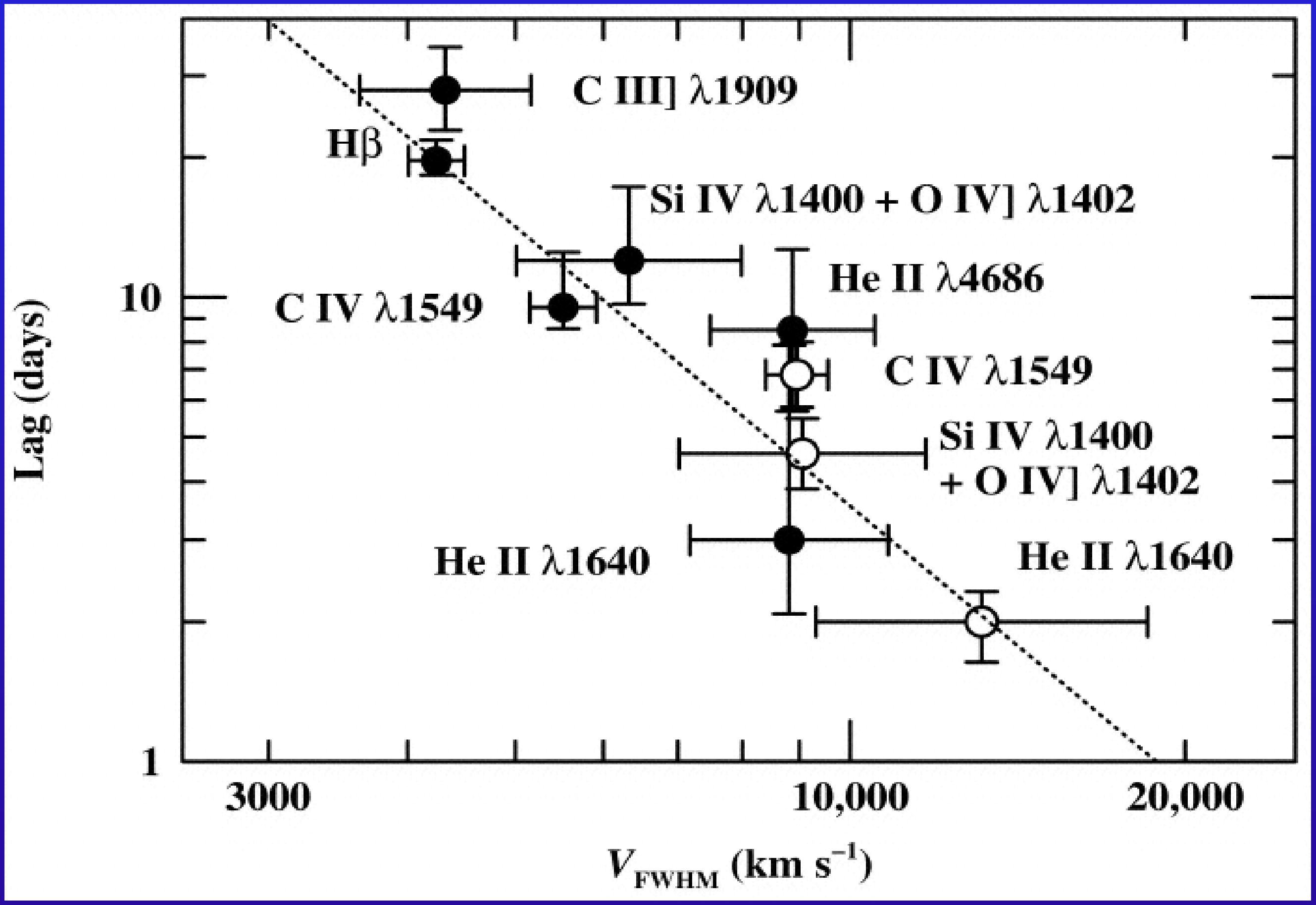

Time lag (CCFs centroids) for various emission lines

Peterson, Wandel, 1999

BLR size and stratification in Mrk110

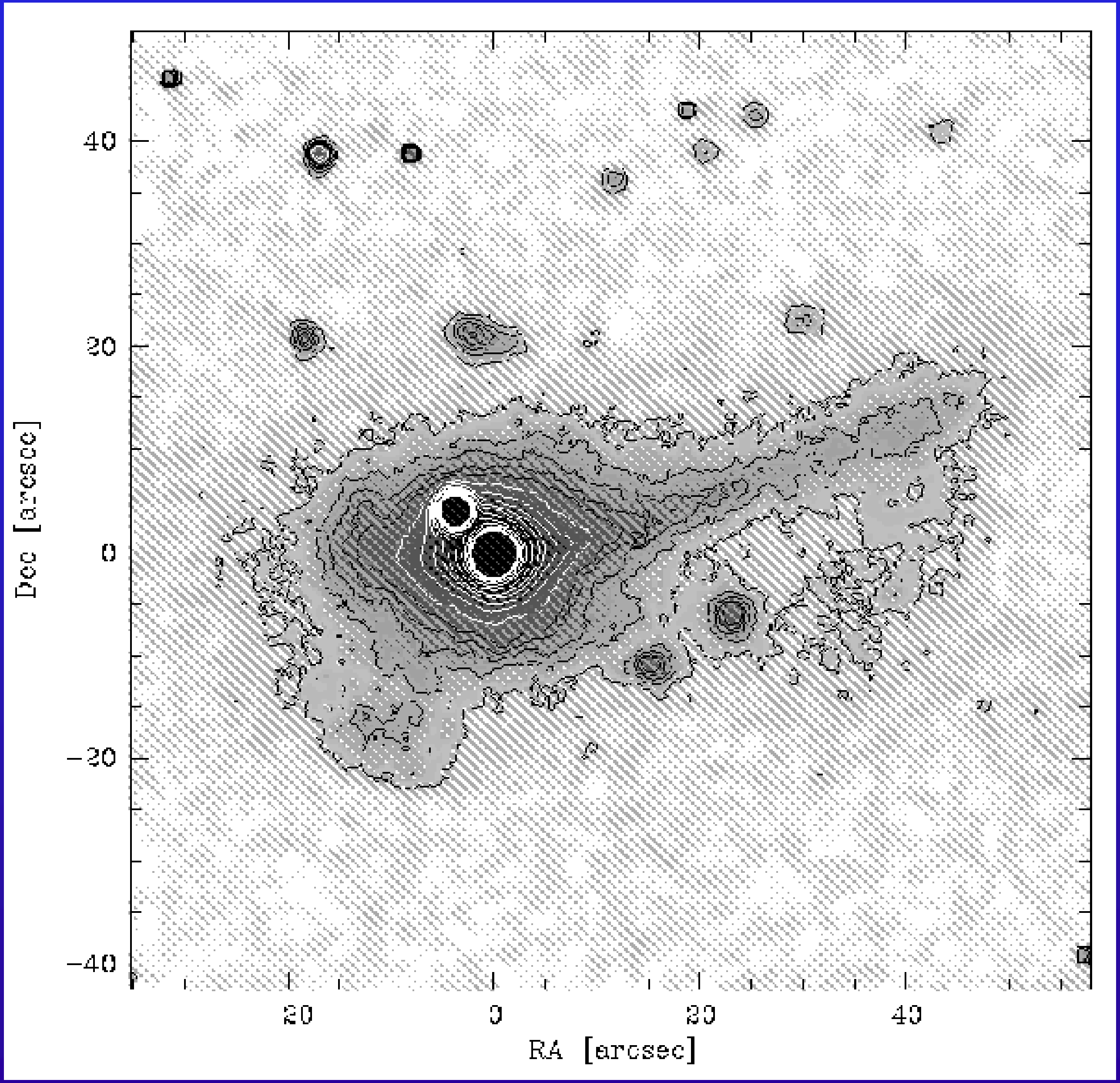

Mrk110

V = 15.4
M_V = -20.6
z = 0.036
FWHM(Hβ)=1680 km s^{-1}

tidal arm: 35kpc

HET variability campaign of Mrk110

long-term continuum light curve

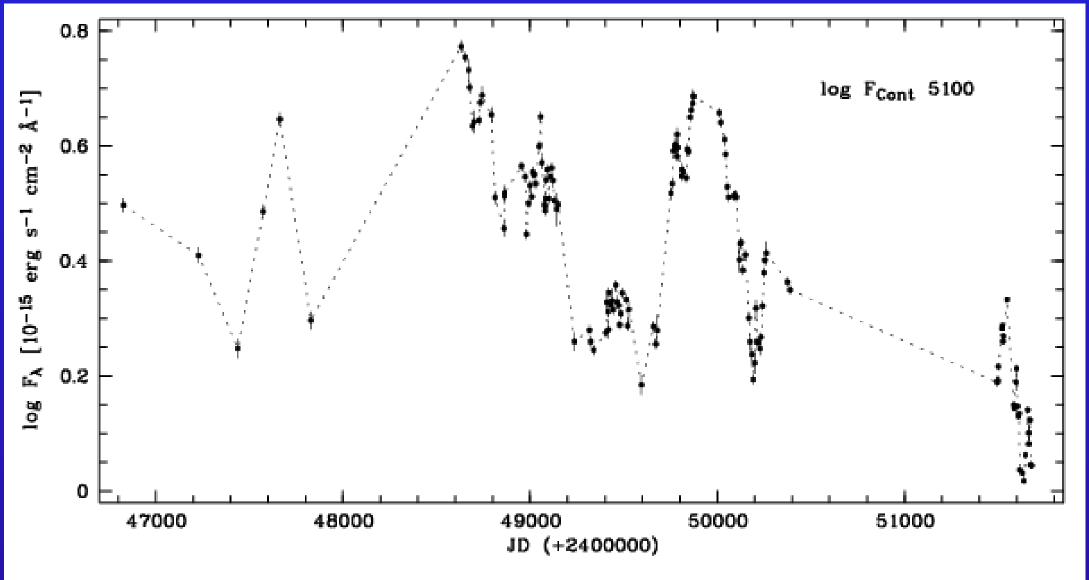

1987

2000

Mrk110 spectra taken between 1999 Nov. and 2000 May

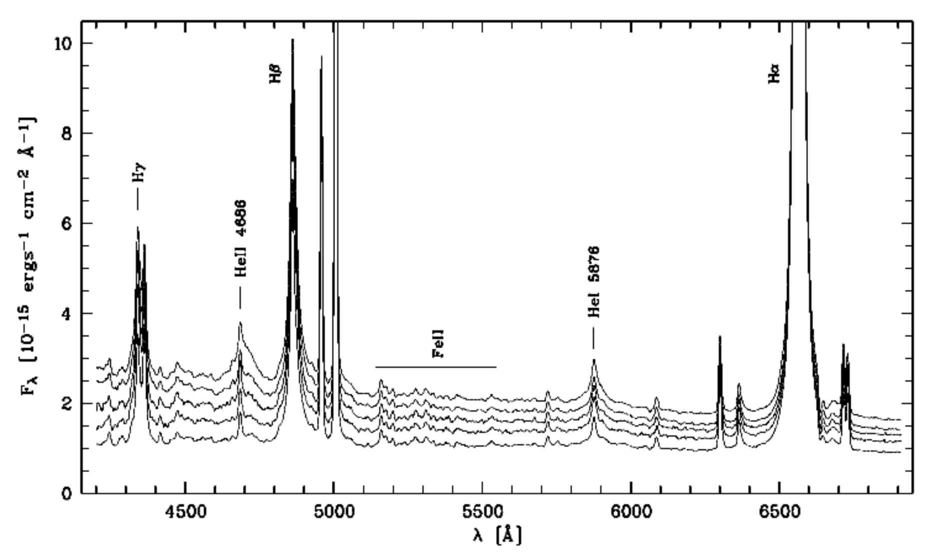

9.2m Hobby-Eberly Telescope at McDonald Observatory
S/N >100

Hobby-Eberly Telescope (HET),McDonald

-Univ. of Texas at Austin
-Pennsylvania State Univ.
-Stanford Univ.
-Göttingen Univ.
-München Univ.

Hobby-Eberly Telescope (HET)

Telescope structure, tracker, and segmented primary mirror

- fixed altitude telescope

- 70 percent of sky observable during specific windows of opportunity

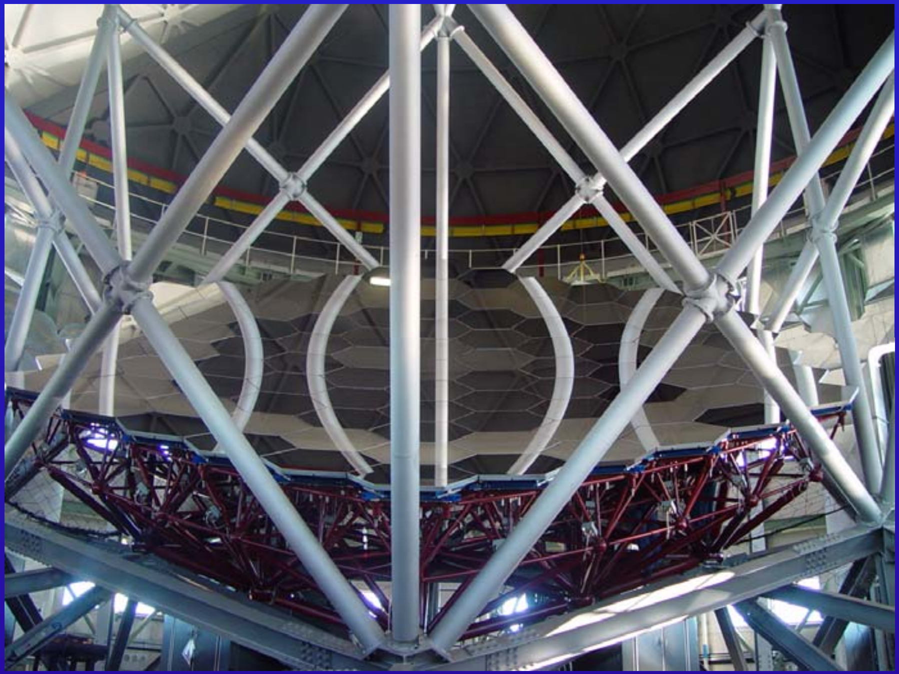

-segm. mirror, diameter: 11 m

-91 mirrors a 1 m diameter

HET variability campaign of Mrk110

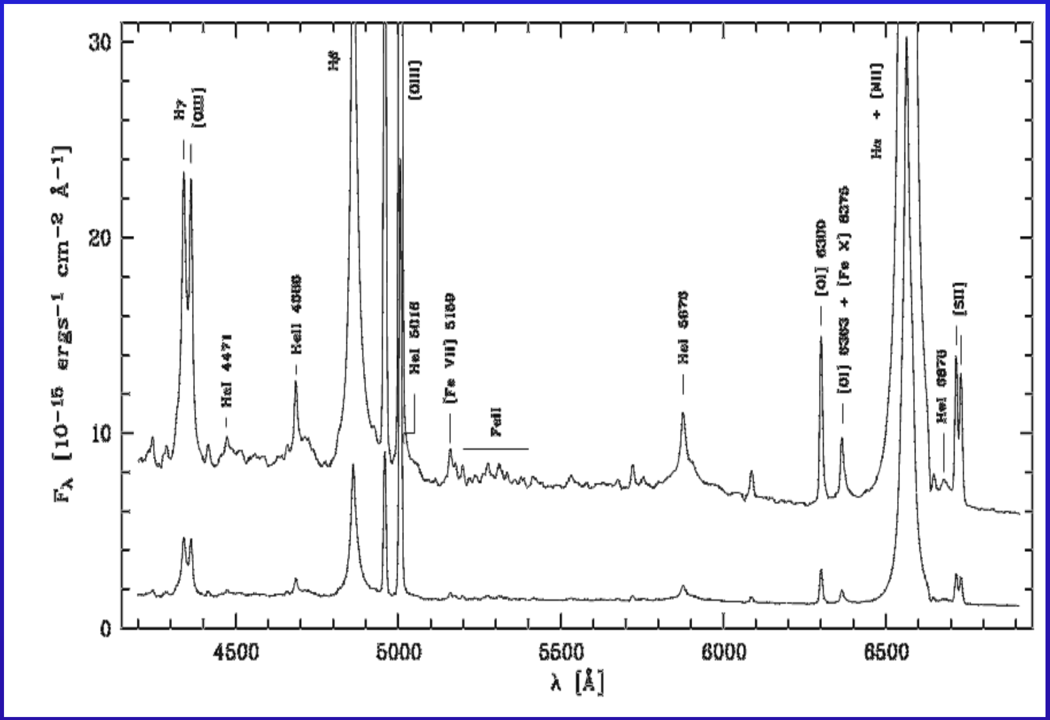

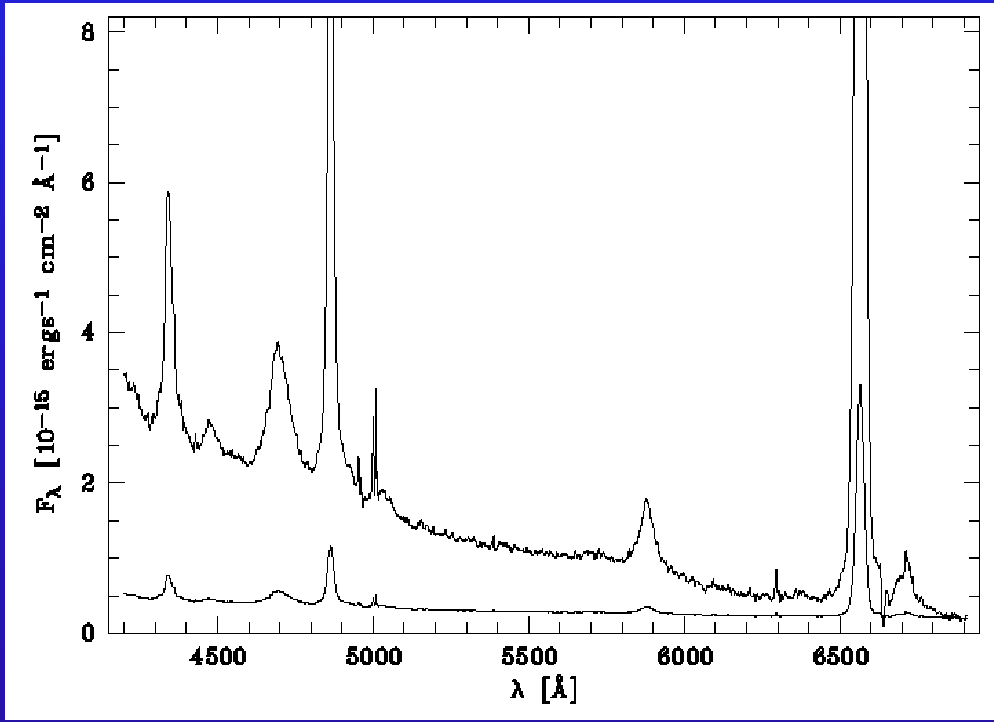

Mean spectrum of Mrk110 for 24 epochs from Nov. 1999 through May 2000

Rms spectrum

- the rms spectrum shows the variable part of the spectrum

Kollatschny et al., 2001

HET variability campaign of Mrk110

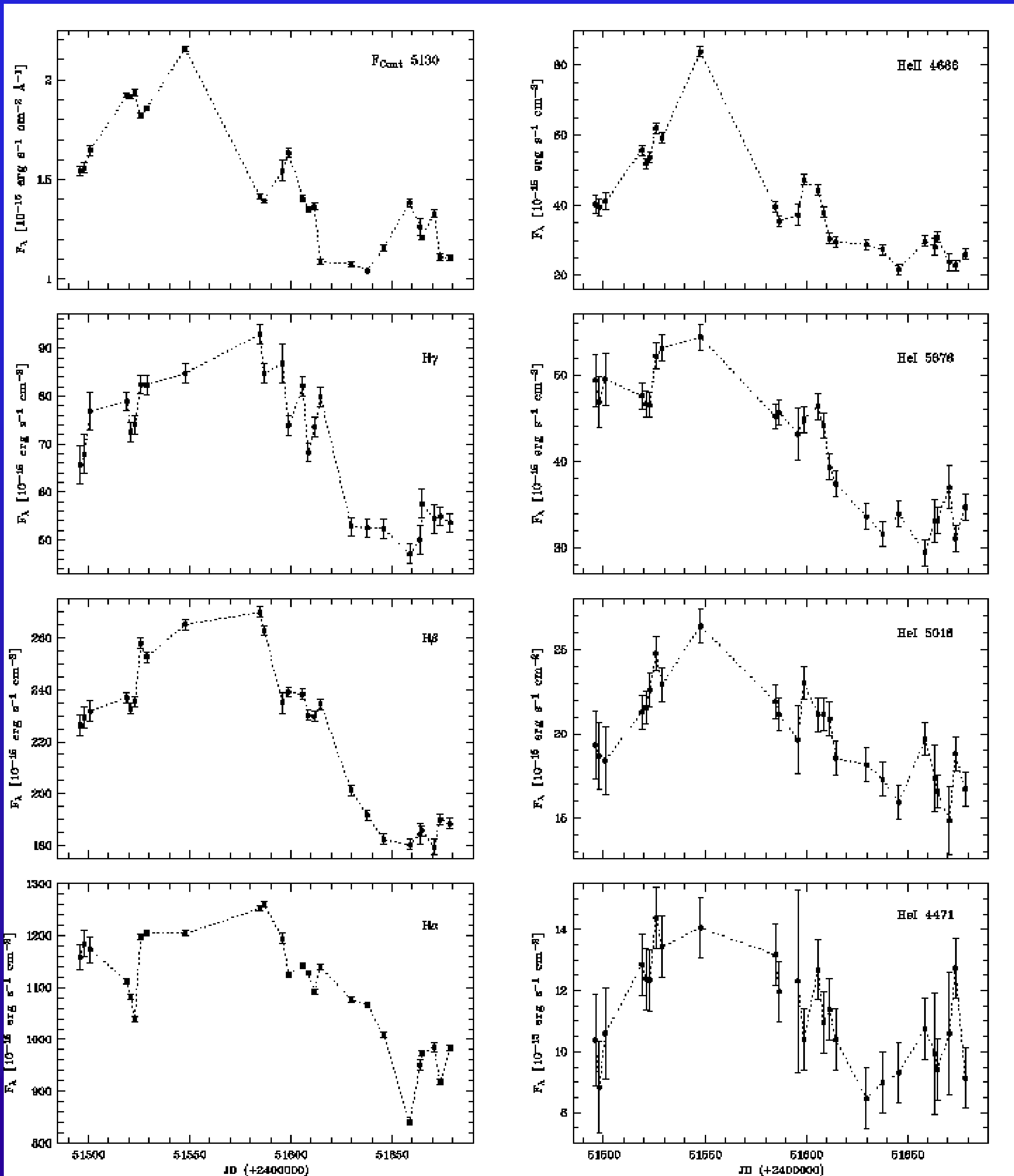

Continuum and integrated emission line (Balmer, HeII and HeI) light curves

1999 Nov. - 2000 May

Kollatschny et al., 2001

BLR size and structure - HET variab. campaign

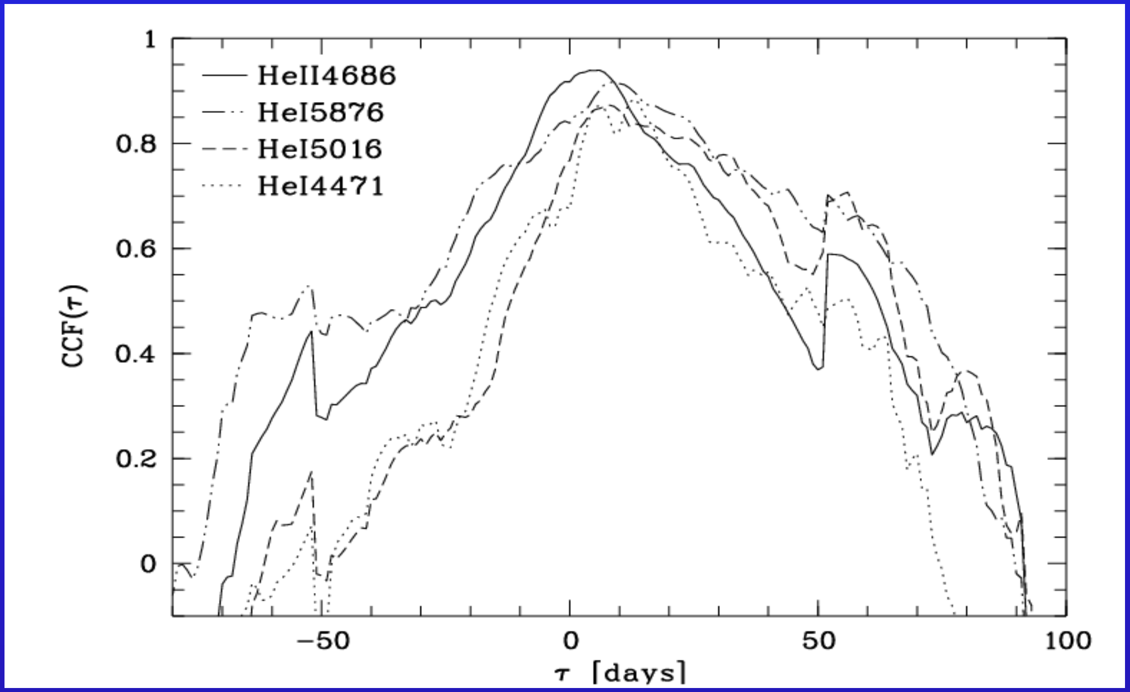

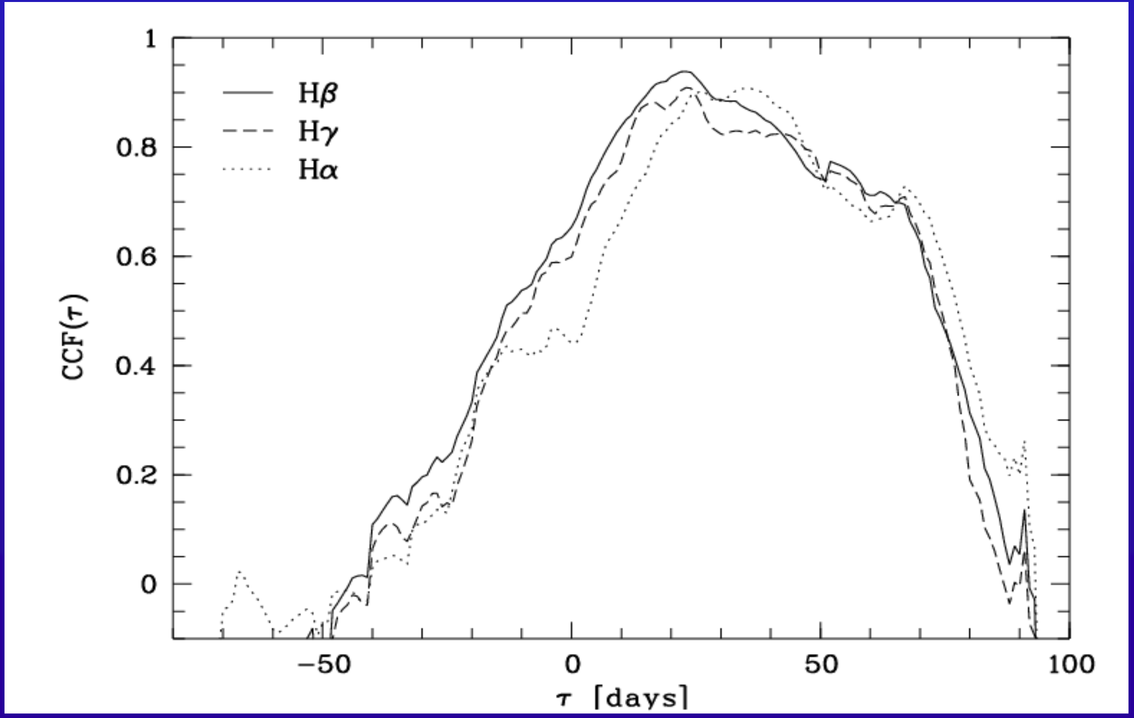

Mkn110

CCF functions of HeII, HeI and Balmer line light curves with continuum light curve.

Line (1)	τ_{cent} [days] (2)
HeIIλ4686	$3.9^{+2.8}_{-0.7}$
HeIλ4471	$11.1^{+6.0}_{-6.0}$
HeIλ5016	$14.3^{+7.0}_{-7.0}$
HeIλ5876	$10.7^{+8.0}_{-6.0}$
Hγ	$26.5^{+4.5}_{-4.7}$
Hβ	$24.2^{+3.7}_{-3.3}$
Hα	$32.3^{+4.3}_{-4.9}$

stratification

BLR size and stratification in Mrk110

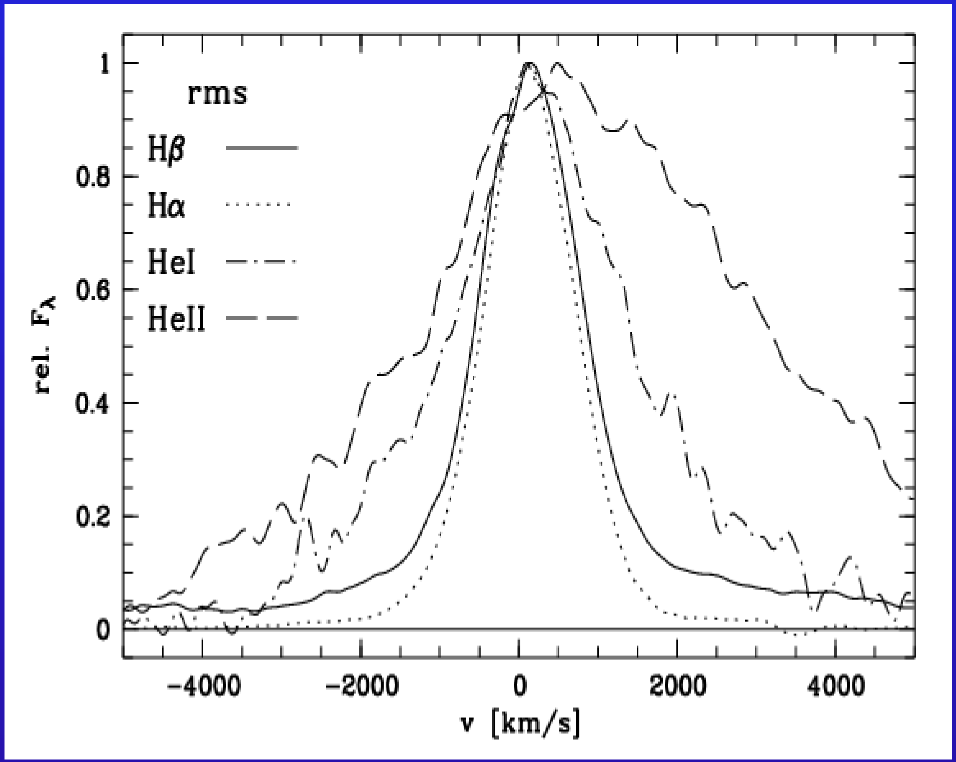

Normalized rms line profiles in velocity space

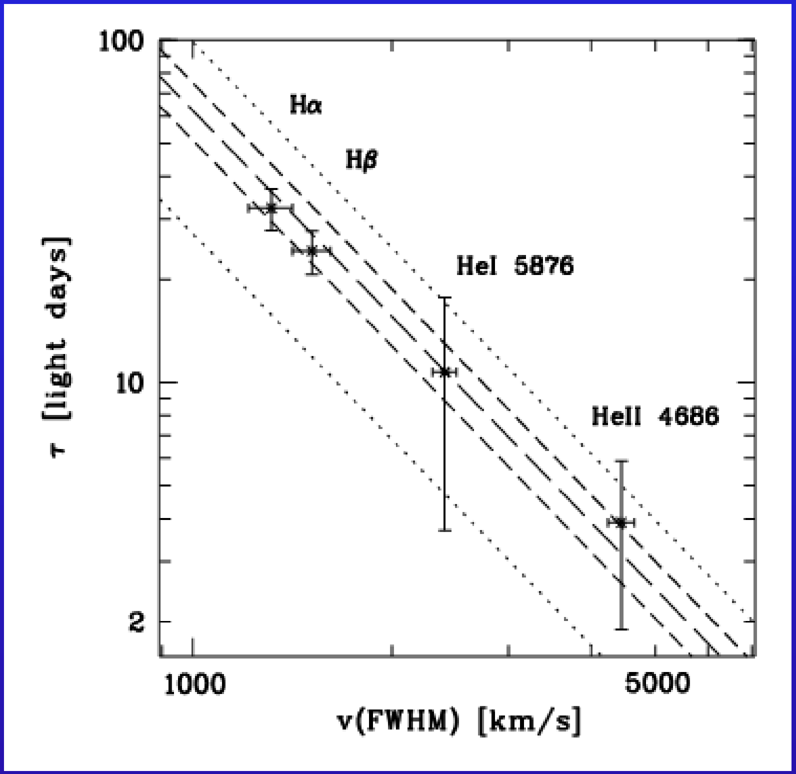

Mean distances of the line emitting regions from central ionizing source as function of FWHM in rms profiles.

The rms spectrum shows the variable part of the spectrum

The dotted and dashed lines correspond to virial masses of .8 - 2.9 $10^7 M_\odot$ (from bottom to top).

Long Term Lightcurve of Mrk926 (1990 - 2005)

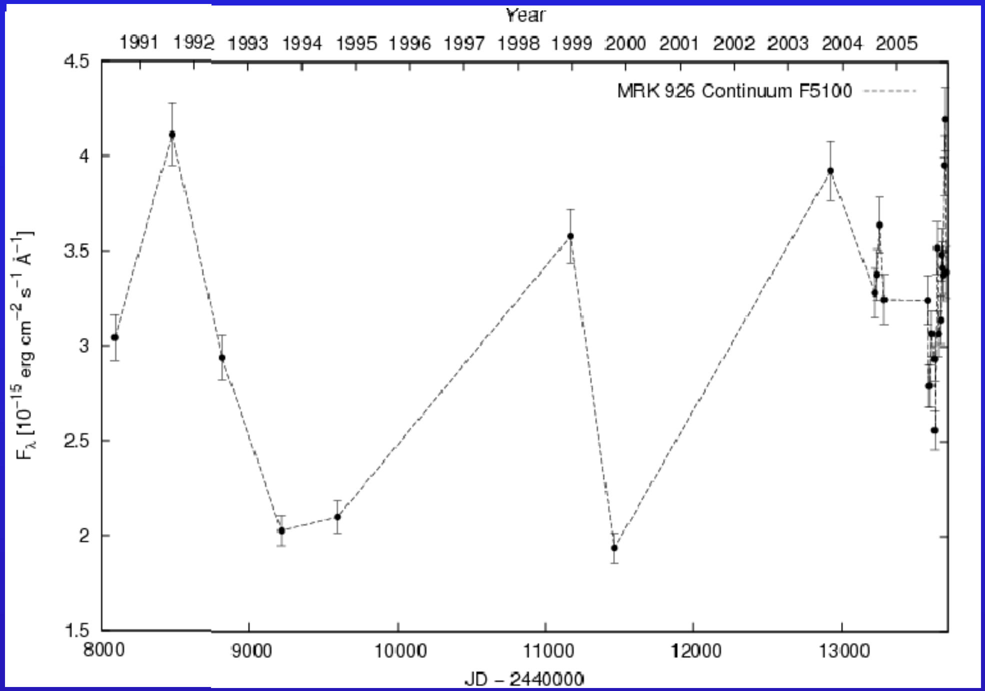

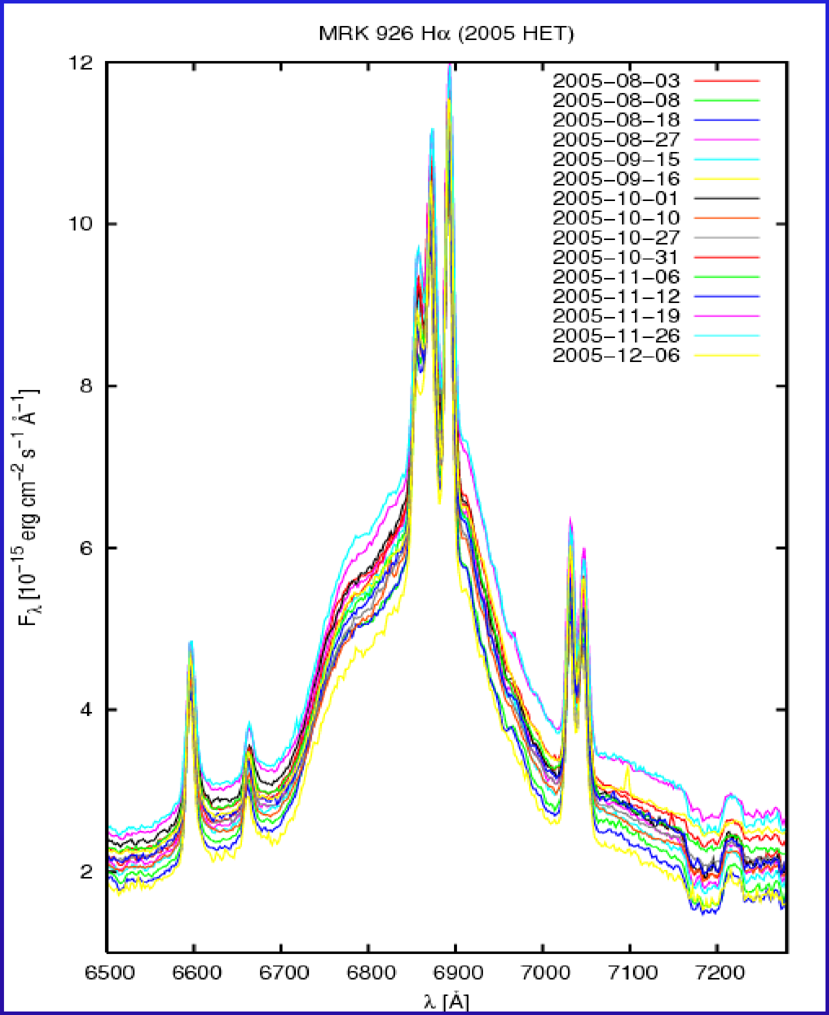

Hα var. in 2005

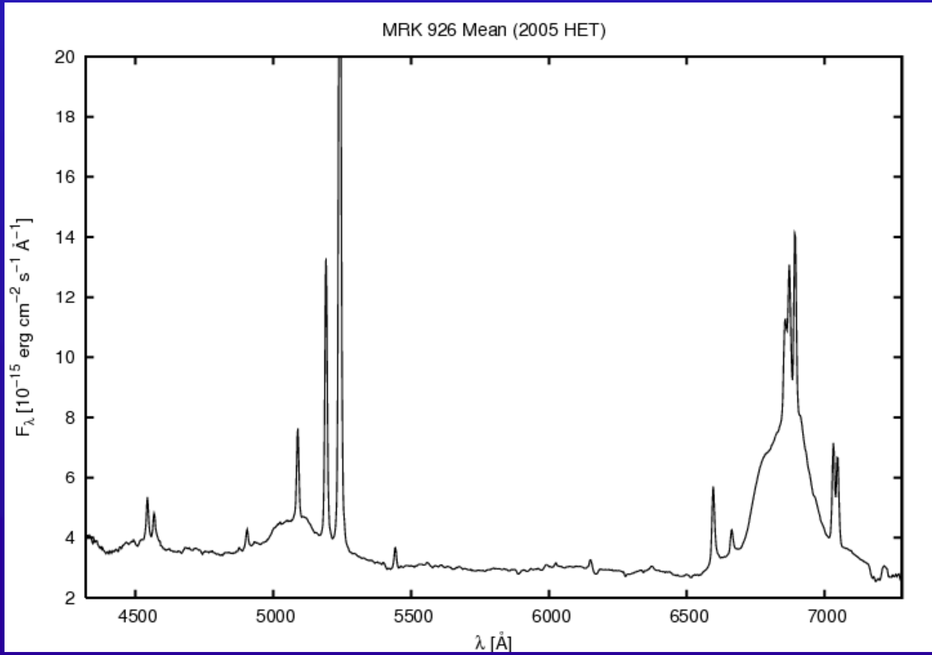

mean spectrum

Lightcurves of Mrk926

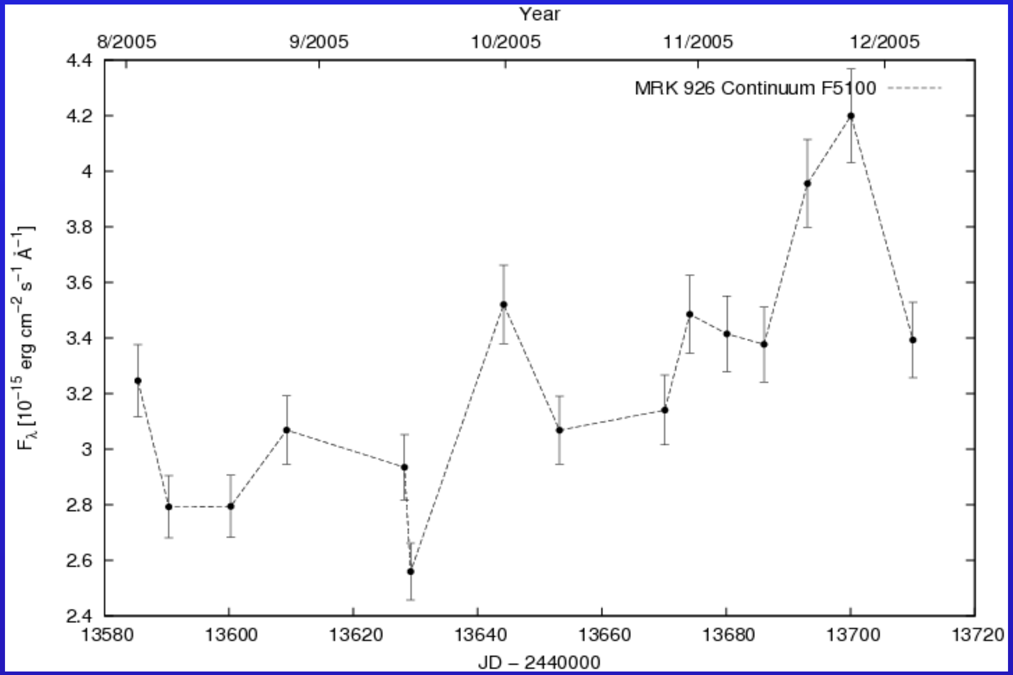

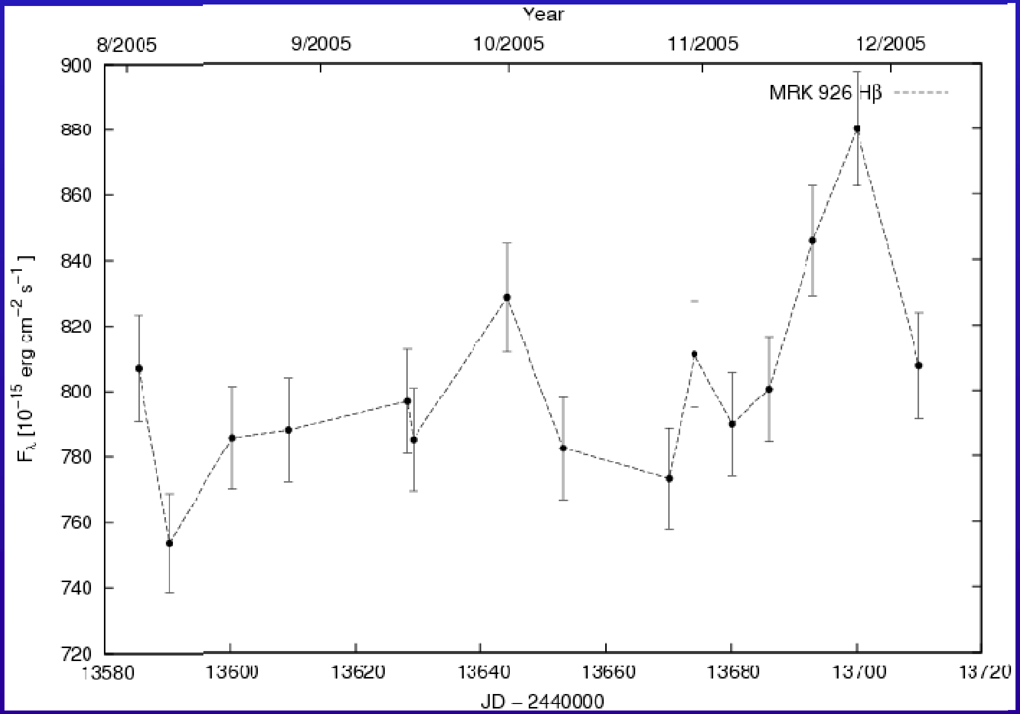

HET var. campaign:
Aug. - Dec. , 2005

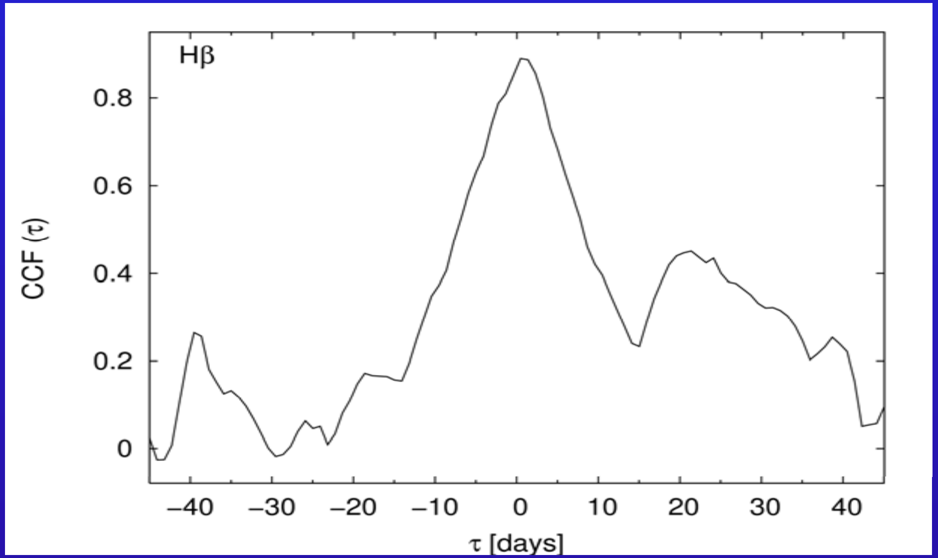

mean distance of Hβ line emitting region: 0.5 ± 2 light days

Hα: 1.5 ± 2. light days

Kollatschny et al., 2007 in prep.

Balmer line averaged BLR size in AGN

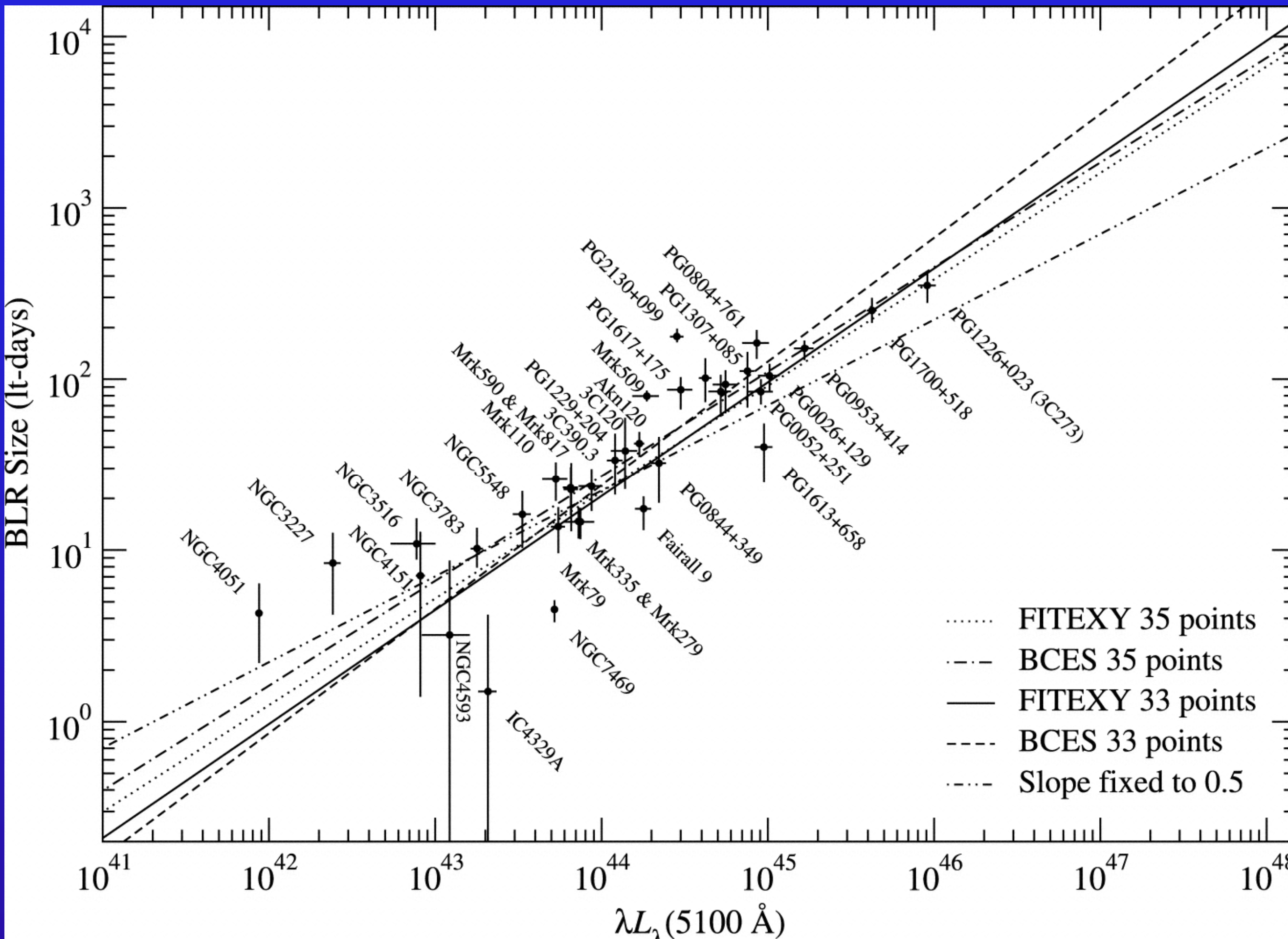

photoion. theory:

$$r = \left(\frac{Q(\mathrm{H})}{4\pi c n_{\mathrm{e}}}\right)^{1/2} \propto L^{1/2}$$

Q = hydrogen-ionizing photons emitted per sec

Relationship between luminosity and broad-line region size
$R_{BLR} \sim L^{0.65}$
But intrinsic scatter due to: BLR density, column density, ionizing spectral energy distribution, ...?

Kaspi et al. 2004

Central Black Hole Mass in Mrk110

Assumption:
emission line clouds
are gravitationally bound
by central object

$$M = \frac{f V_{\rm FWHM}^2 c\tau}{G}$$

cτ = mean dist. of
line em. clouds

V = vel.disp. of clouds
(from rms line width)

f = factor (½ - 5.5)
(unknown geometry
and kinematics)

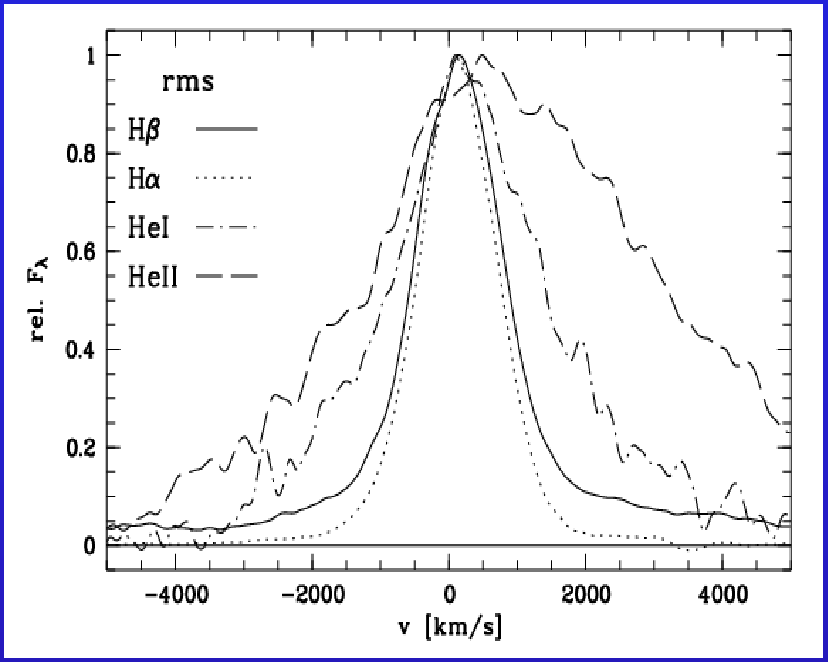

Normalized rms line profiles in velocity space

Line (1)	FWHM(rms) $[\mathrm{km\ s^{-1}}]$ (2)	τ_{cent} [days] (3)	M $[10^7 M_\odot]$ (4)
HeIIλ4686	4444. ± 200	$3.5^{+2.}_{-2.}$	$2.25^{+1.63}_{-0.45}$
HeIλ5876	2404. ± 100	$10.8^{+4.}_{-4.}$	$1.81^{+1.36}_{-0.33}$
Hβ	1515. ± 100	$23.5^{+4.}_{-4.}$	$1.63^{+0.33}_{-0.31}$
Hα	1315. ± 100	$32.5^{+4.}_{-4.}$	$1.64^{+0.33}_{-0.35}$

Kollatschny et al., 2001, 2003

Central Black Hole Mass in Mrk926

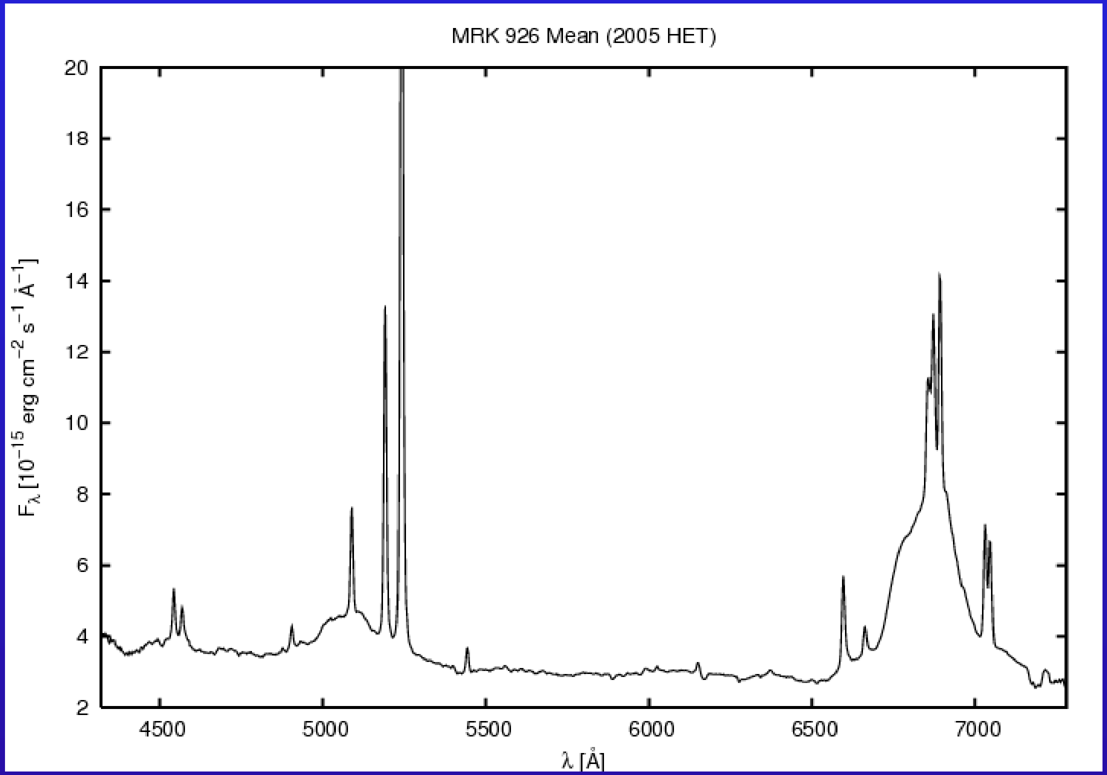

cτ = mean dist. of Hβ line emitting region: 0.5 light days

v = vel.disp. of clouds (from line width) ~ 8 000 km/s

$1.1 \cdot 10^7 M_O$ (f=1.5)

Central Black Hole Masses in AGN

Black hole mass vs. luminosity for AGN

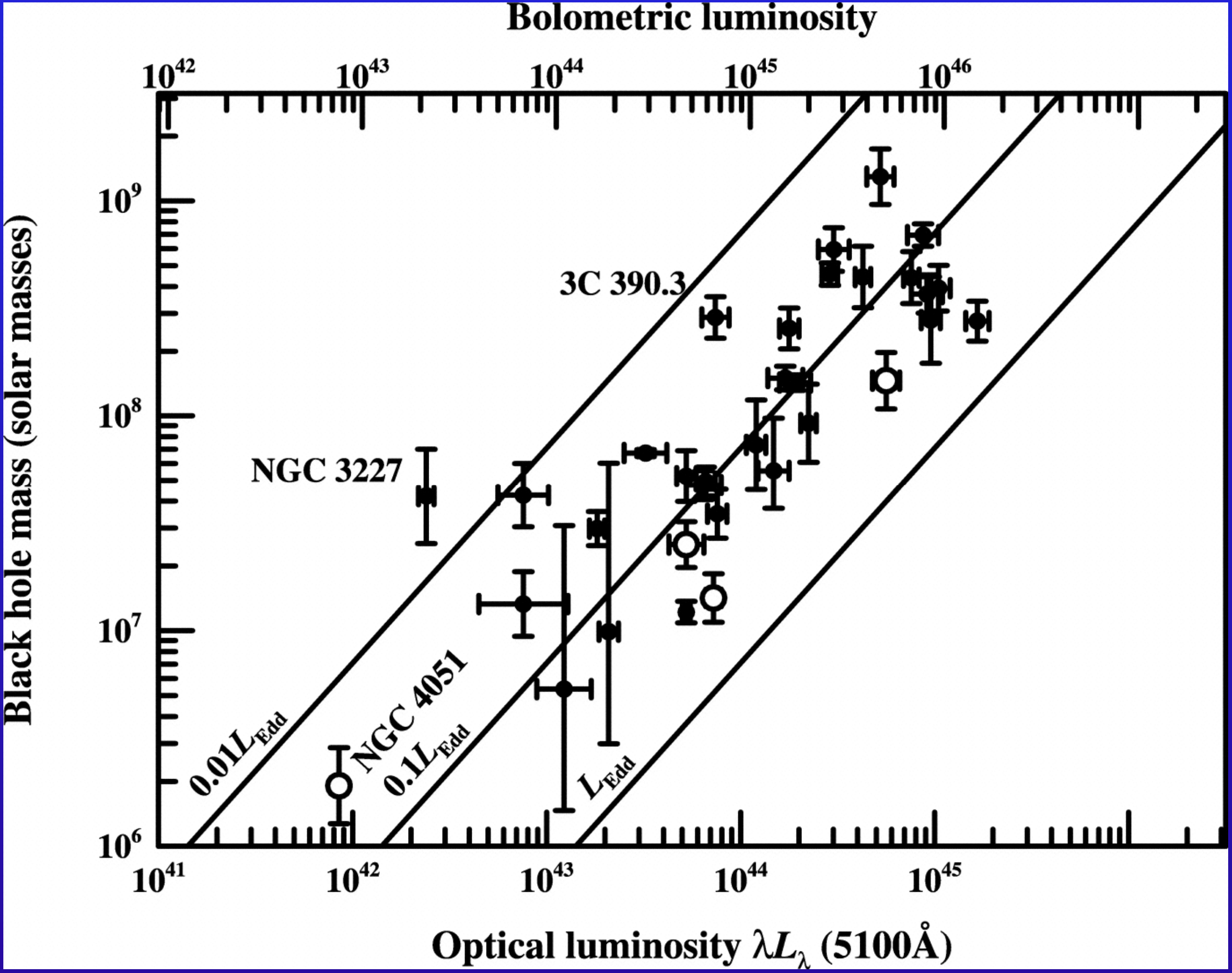

BH mass for 35 reverberation mapped AGN.

--- : lines of constant mass to luminosity ratio
open circles: NLSy1

Peterson et al., 2004

BLR Kinematics: Idealized Model

Influence of BLR motions on line profile variations

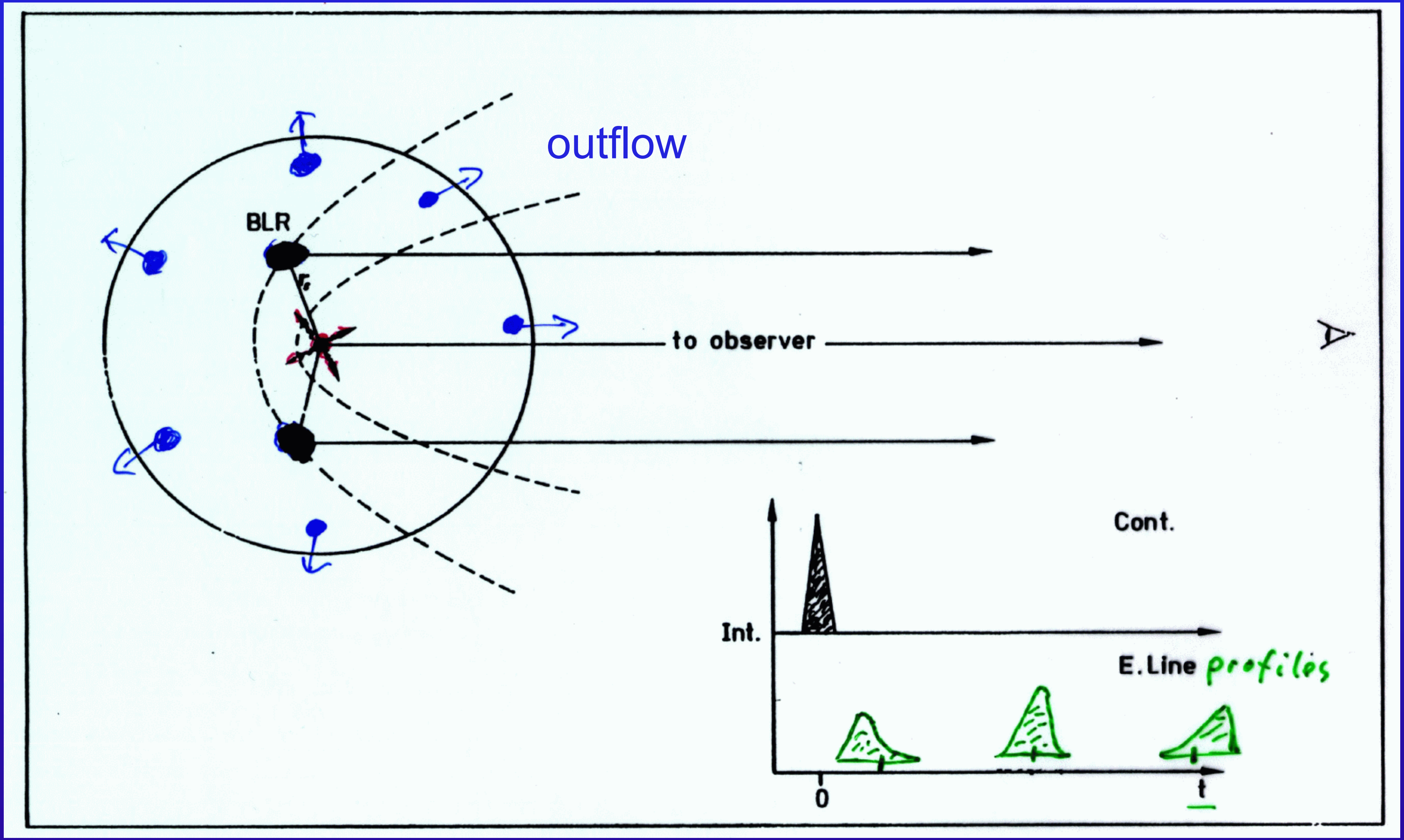

Theory : BLR kinematics - line profile variations

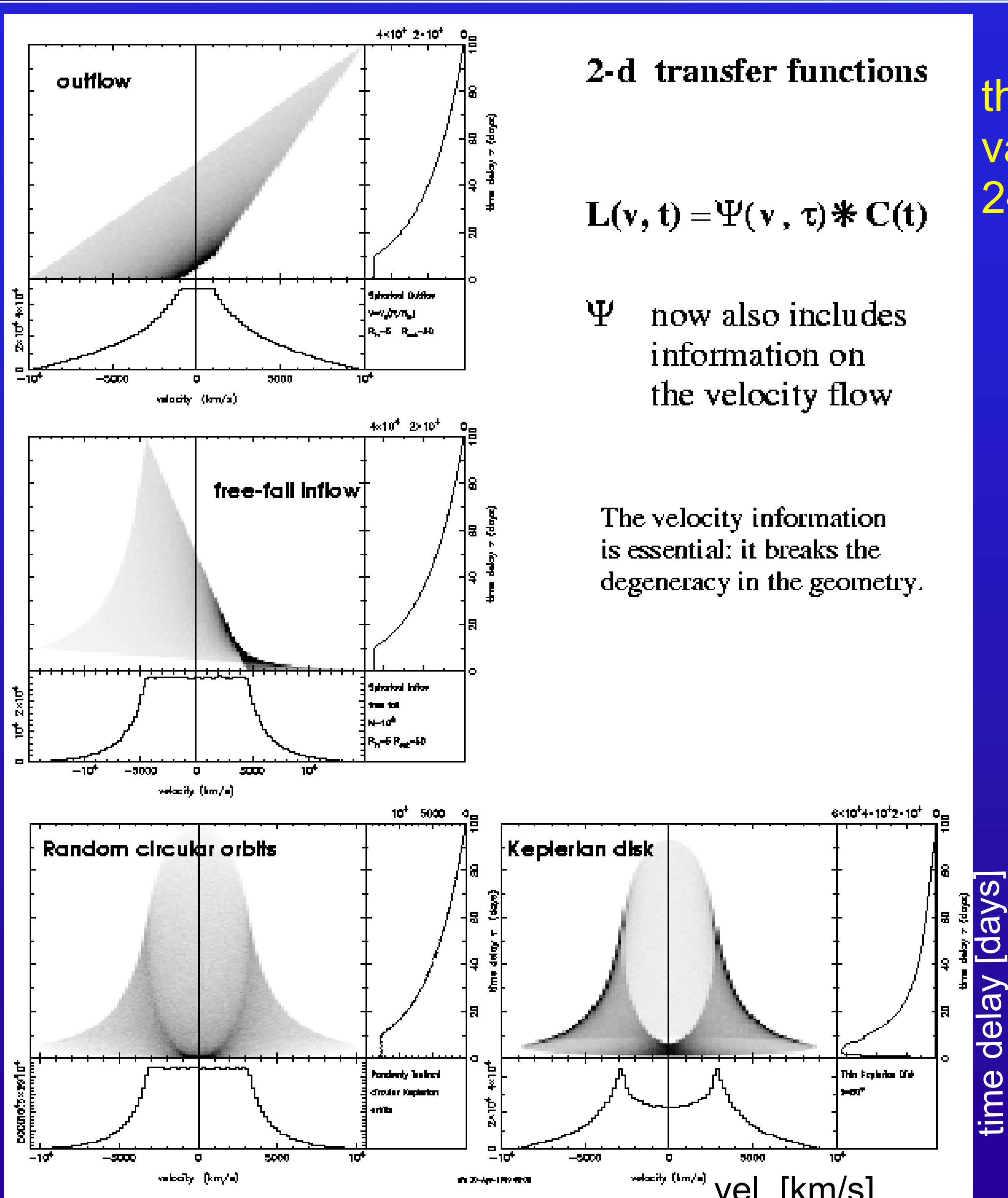

2-d transfer functions

$$L(v, t) = \Psi(v, \tau) * C(t)$$

Ψ now also includes information on the velocity flow

The velocity information is essential: it breaks the degeneracy in the geometry.

theoretical emission line profile variations to derive
2-dim. velocity-delay maps ψ

velocity-delay maps for different flows

Welsh & Horne, 1991
Horne et al., 2004

BLR kinematics and accretion disk structure

Mean Hβ line profile of Mrk110 in velocity space

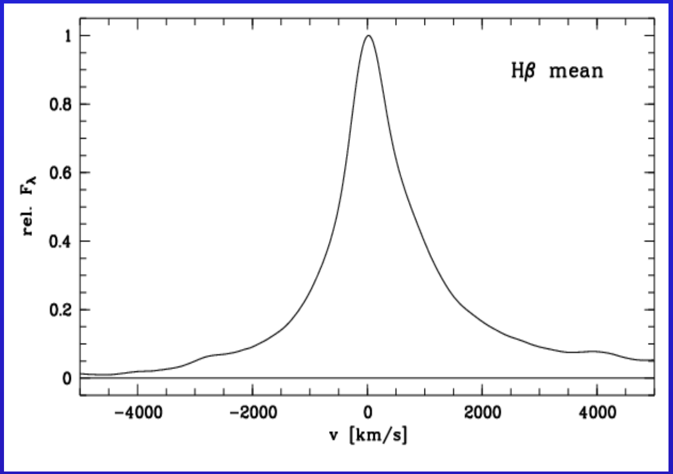

Light curves of the continuum, of the Hβ line center, and of different blue and red line wing segments

Δv = 400 km/s

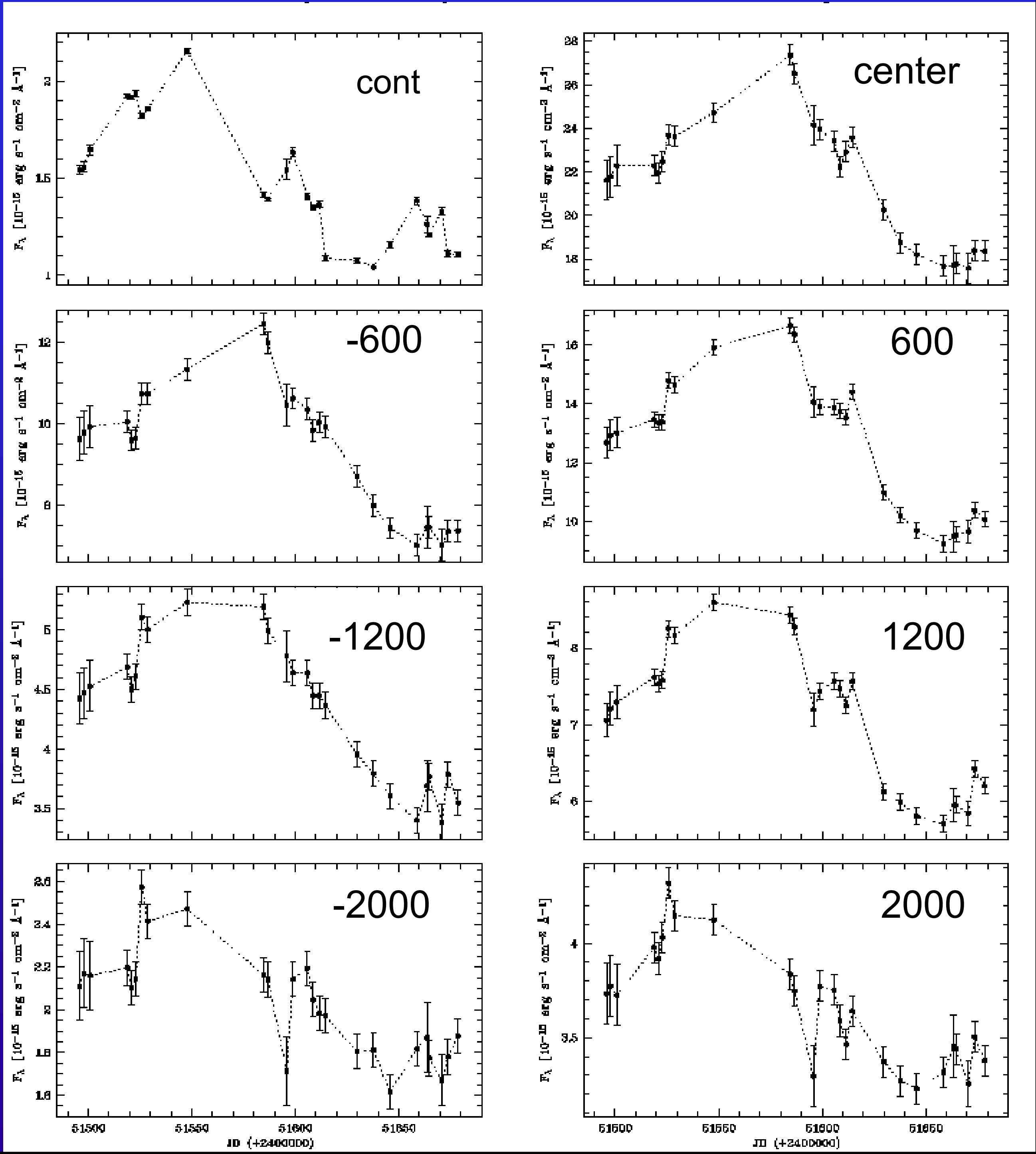

Kollatschny & Bischoff 2002

BLR: Accretion disk structure in Mrk110

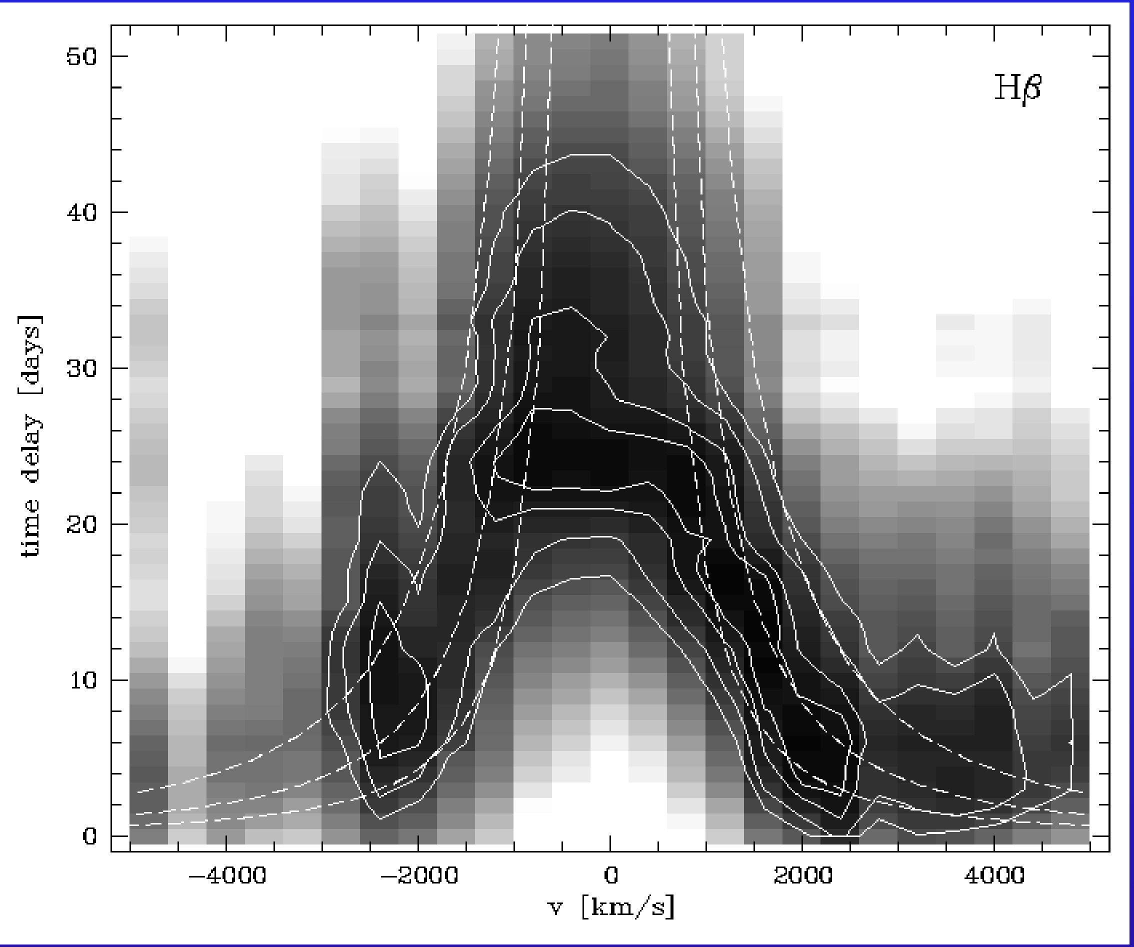

Velocity-delay map

Kollatschny 2003a

2-D CCF : correlation of Hβ line profile segments with cont. variations (grey scale)

Contours of correlation coefficient at levels of .85 to .925 (solid lines).

Dashed curves: theoretical escape velocity envelopes for masses of 0.5, 1., 2. 10^7 $M_\odot$ (from bottom to top).

E
c
h

Echo image

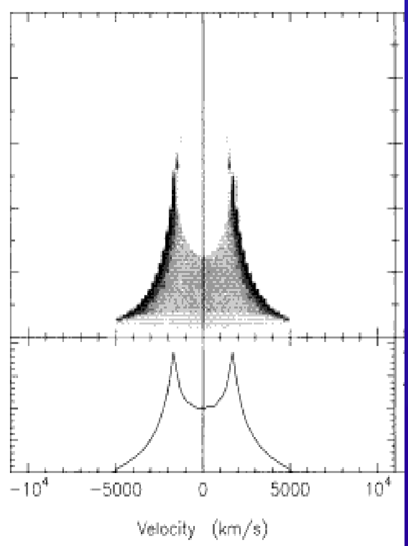

Theoretical velocity-delay maps for different flows:
Keplerian disk BLR model: fast response of both outer line wings

Welsh & Horne 1991, Horne et al. 2004

Velocity-delay maps: accretion disk structure

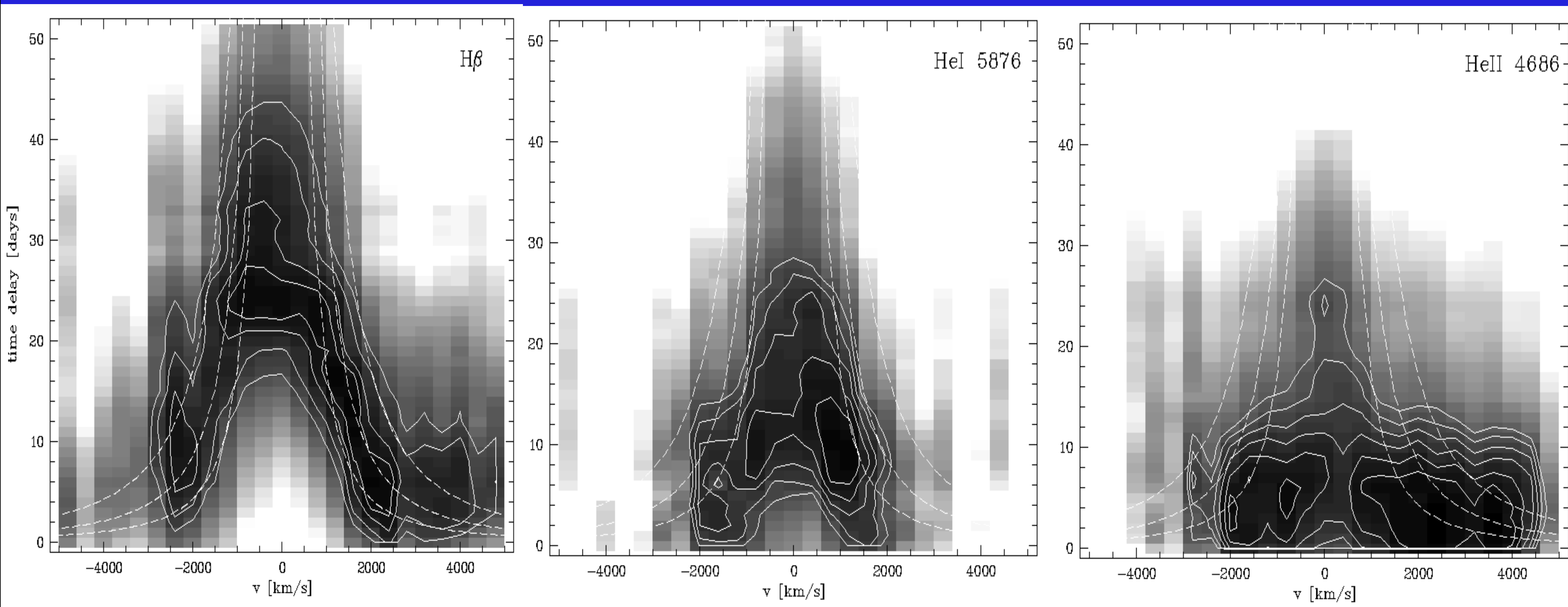

2-D CCF : correlation of Hβ, HeI, HeII line profile segments with continuum variations (grey scale).

Kollatschny 2003

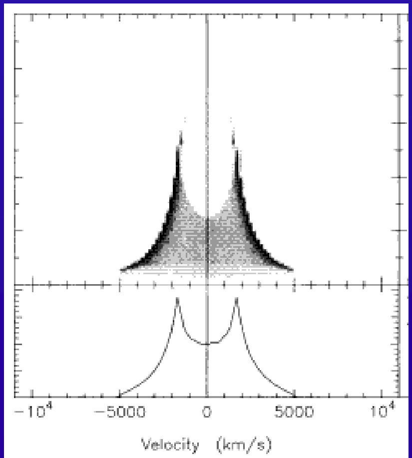

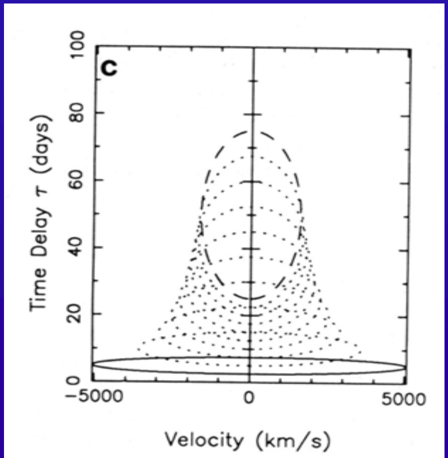

Keplerian disk BLR model: fast response of both outer line wings

Solid line: innermost radius at 5 ld

BLR: Accretion disk wind in Mrk110

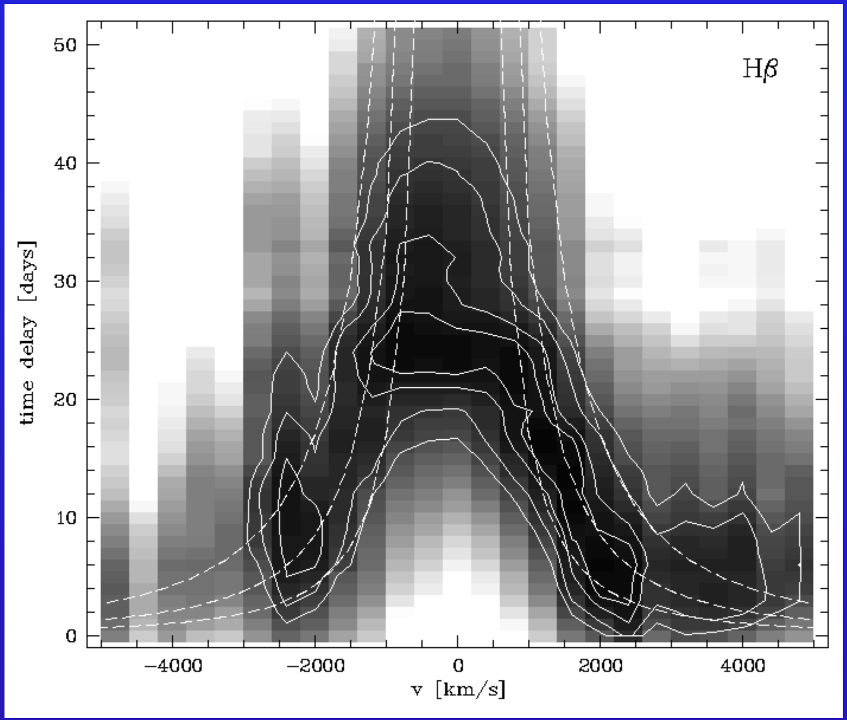

2-D CCF: velocity-delay map

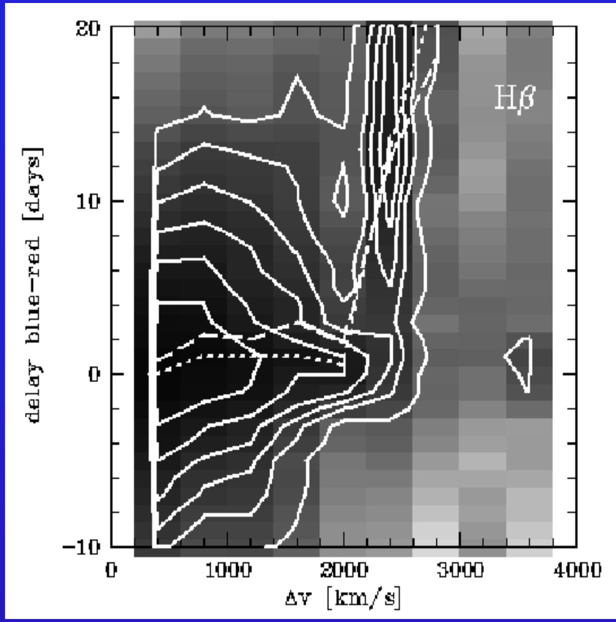

Time delay of blue line wing to red line wing as function of dist. to line center

Outer line wings: inner BLR

Disk wind model of BLR: Slightly faster and stronger resonse of red wing

Chiang & Murray, 1996

Disk driven outflow models compared to spherical wind models:
velocity decreases with radius (rather than the other way around)

Koenigl & Kartje, 1994

BLR Structure and Kinematics in Mrk110

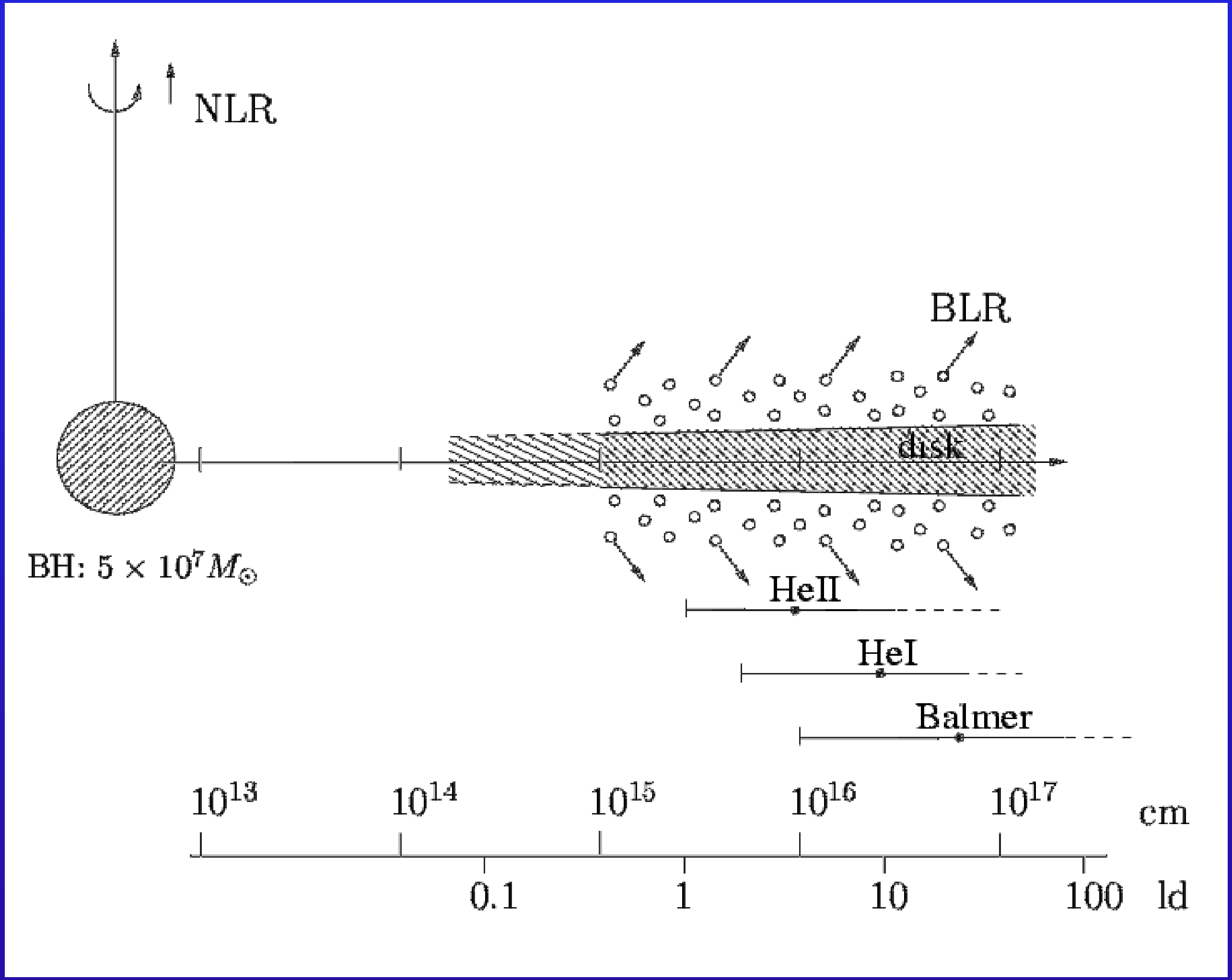

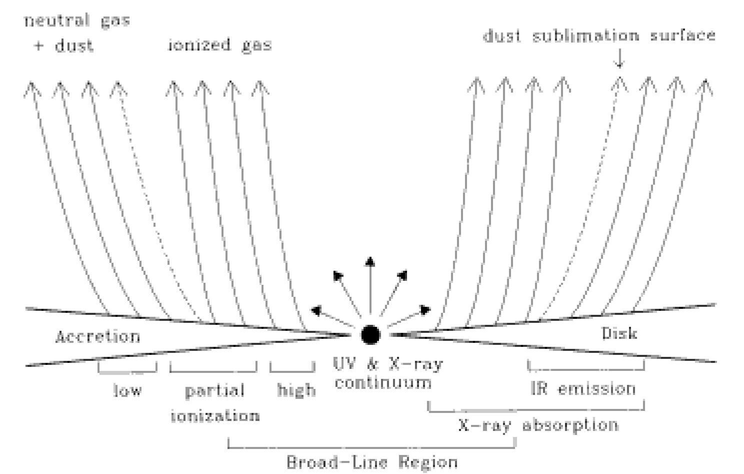

FIG. 13.—Schematic representation of how a disk-driven hydromagnetic wind, which is characterized by a highly stratified density distribution, interacts with the active galactic nucleus (AGN) continuum emission. The innermost regions are heated and ionized by the powerful radiation field, with the temperature and degree of ionization varying both with distance and with the polar angle, whereas the outer regions (beyond the dust sublimination radius) are cooler and contain dust. The radiation pressure force on the dust causes the outer streamlines to have a larger opening angle.

Koenigl & Kartje 1994

accretion disk wind in Mrk110

Kollatschny 2003a

Gravitational Redshift in Mrk110 Line Profiles

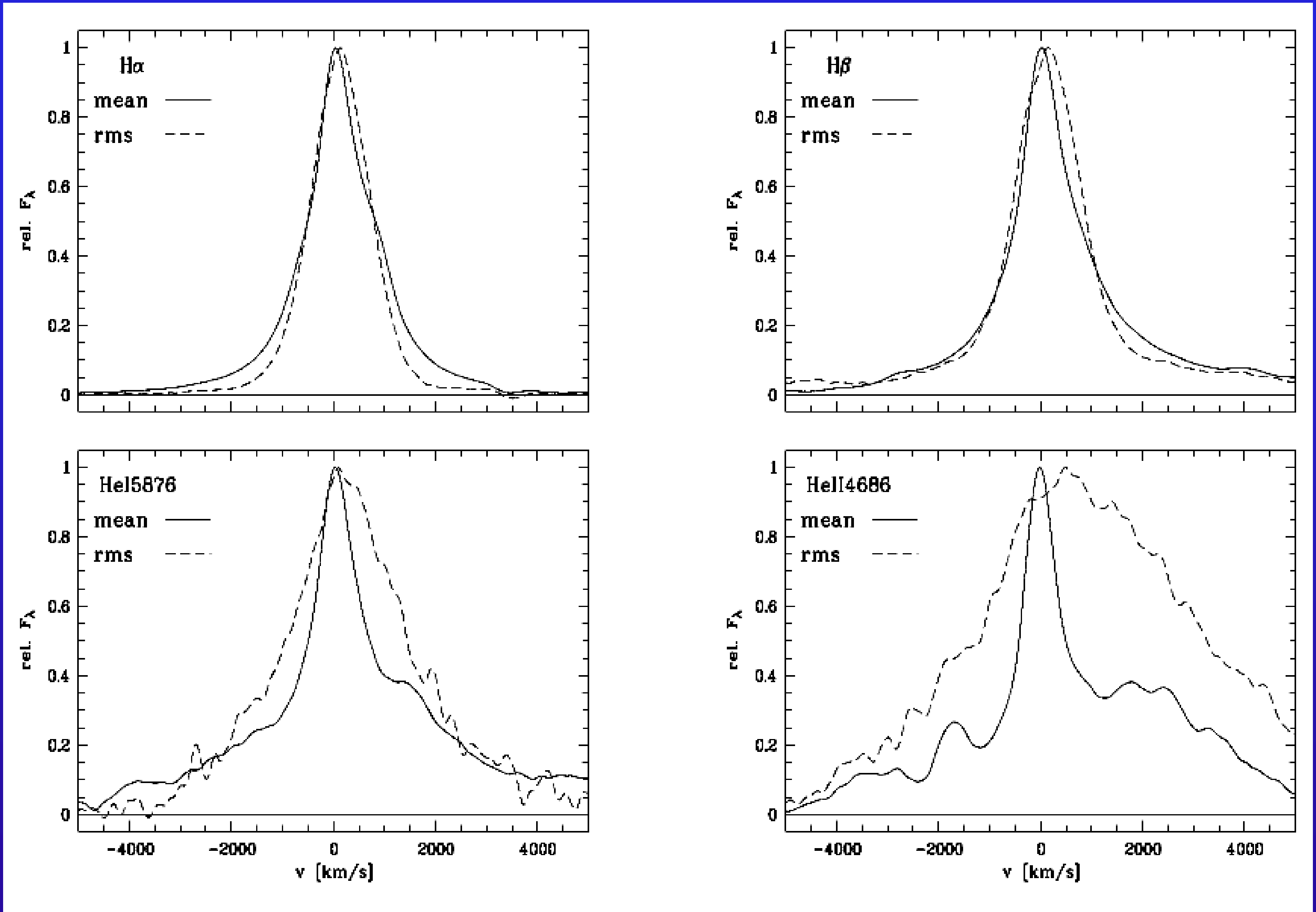

Normalized mean and rms Balmer and He emission line profiles

Kollatschny, 2003b

Central Black Hole Mass M(grav) in Mrk110

Measurements of gravitational redshift:

Observed shift of rms profiles identified as gravitational redshift.

$$M_{grav} = c^2 G^{-1} R \Delta z.$$

R=cτ = mean distance of line em. clouds

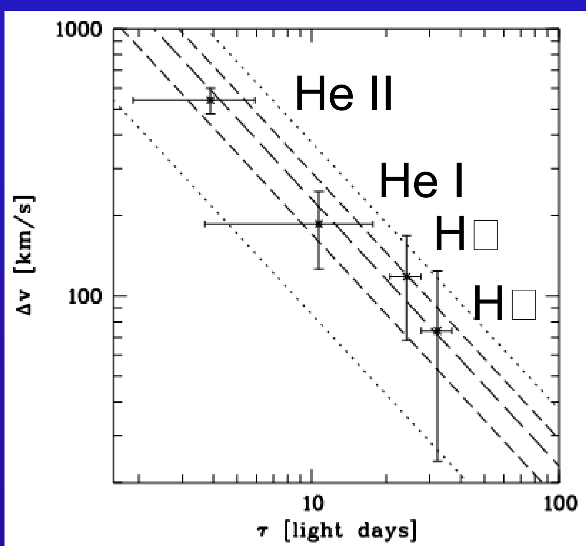

Line	FWHM(rms) [km s^{-1}]	$\Delta\, v_{cent}$(rms) [km s^{-1}]	τ [days]	M_{grav} [$10^7 M_\odot$]
(1)	(2)	(3)	(4)	(5)
HeII	4444. ± 200	541. ± 60	3.9 ± 2.	13. ± 3.
HeI	2404. ± 100	186. ± 60	10.7 ± 6.	12. ± 4.
Hβ	1515. ± 100	118. ± 50	24.2 ± 4.	17. ± 4.
Hα	1315. ± 100	74. ± 50	32.3 ± 5.	14. ± 5.

$$M_{grav} = 14. \pm 3 \cdot 10^7 M_\odot.$$

Line shift vs. distance

Dotted and dashed curves: computed lines of gravitational redshift for masses of 5. - 22. $10^7 M_O$ (from bottom to top).

XMM (RGS) Spectrum of Mrk110

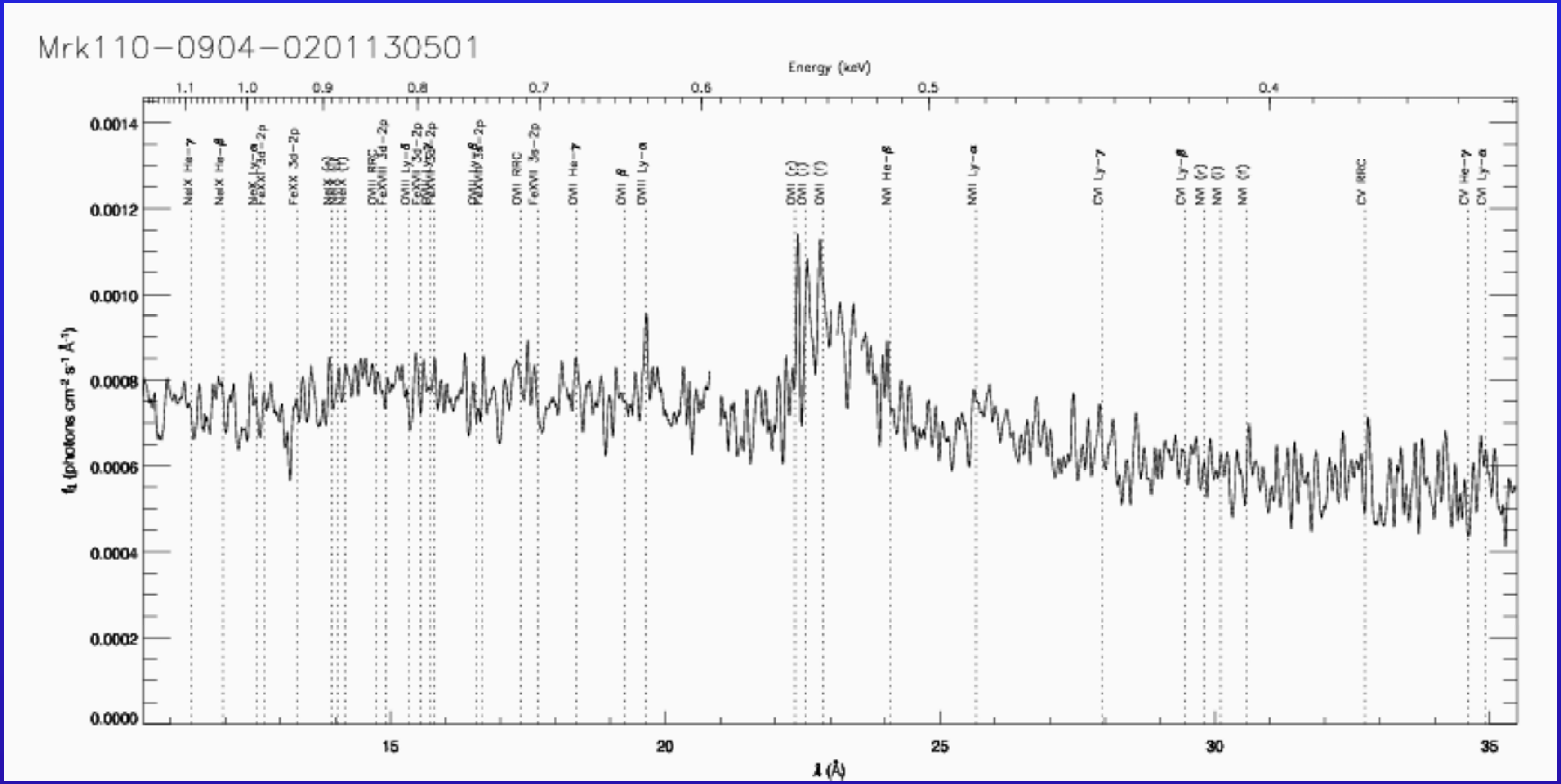

Smoothed fluxed RGS spectrum of Mrk110. The energies at which the most common mission lines should lie are marked with vertical dashed lines.

Broad relativistic OVII emission ($\Delta v \approx 6990$ km/s)

Boller,Balestra,Kollatschny 2007

Gravitational Redshift in Mrk110

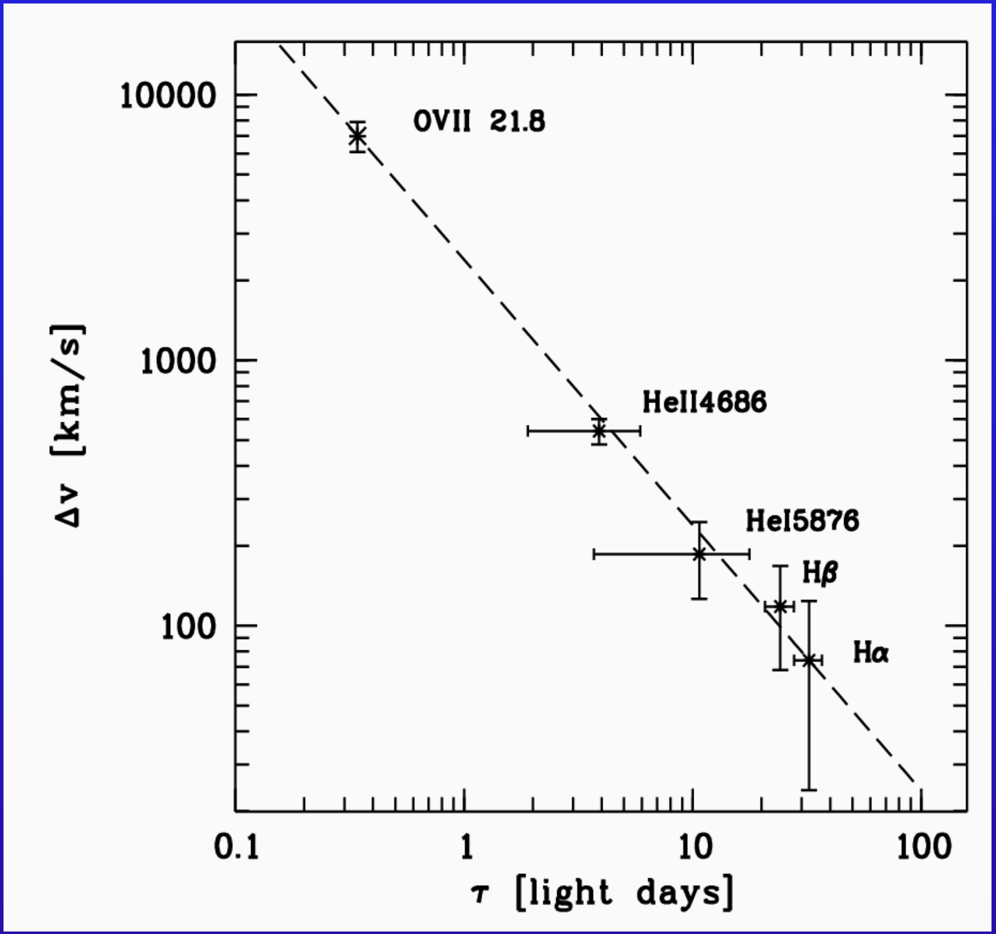

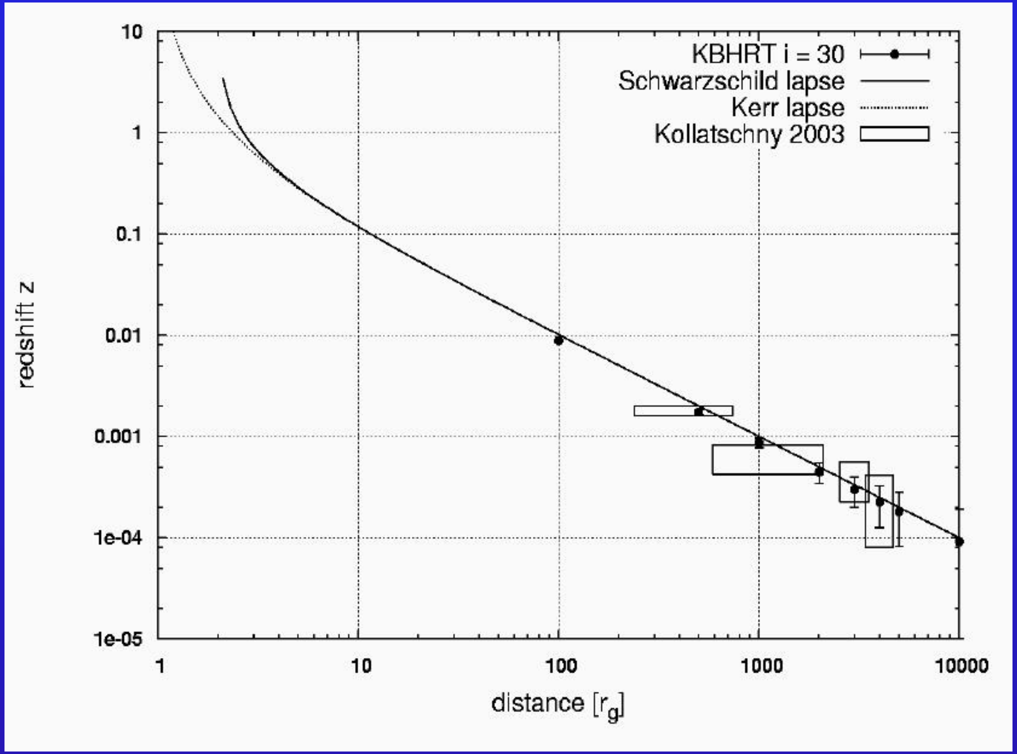

Fig. 9. Synoptical plot with optical K03 data for Mrk 110 (*boxes*) and best fitting Kerr ray tracing simulation with $i \sim 30°$ (*filled circles*) as well as lapse functions for a static (Schwarzschild, *solid*) and rotating (Kerr, *dotted*) black hole. An essential statement illustrated here is that optical BLR lines can **not** probe black hole rotation due to their huge distance. Generally, multi–wavelength observations are recommended to fill the gap at smaller radii.

Relativ. line shift vs. distance

OVII: 0.34 ld

Mueller & Wold 2006

Inclination angle i of accretion disk in Mrk110

$$M_{orbital} = f v^2 G^{-1} R$$

$$M_{grav} = c^2 G^{-1} R \Delta z.$$

$$M_{orbital} = 1.8 \pm 4 \cdot 10^7 M_\odot$$

$$M_{grav} = 14. \pm 3 \cdot 10^7 M_\odot$$

$$M_{orbital}/M_{grav} = sin^2 i.$$

Inclination i = 21 ± 10 deg

Kollatschny 2003b

The inner BLR structure in Mrk110

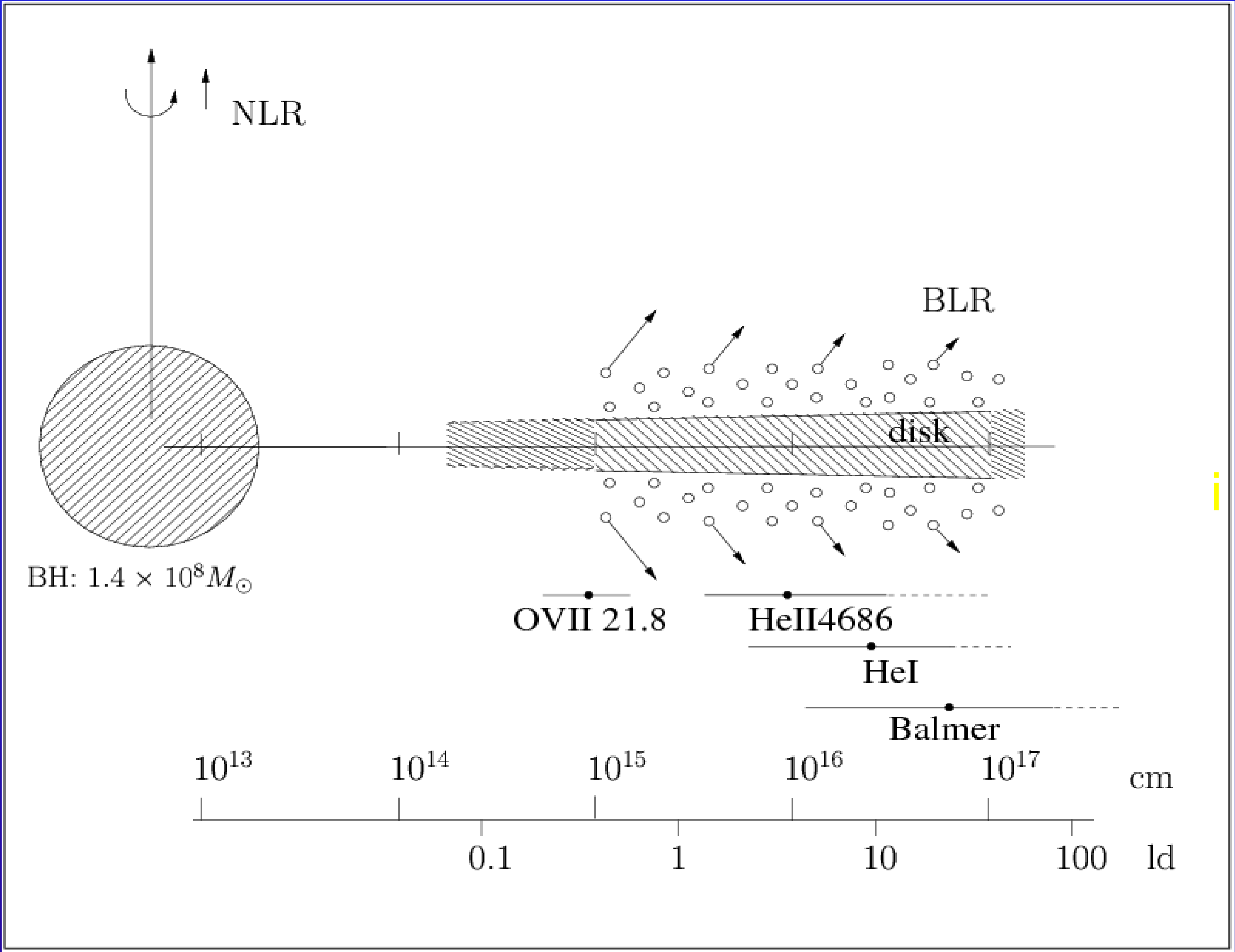

i = 21°±10

opt.: 3.9 light-days ($\hat{=}$ 9.8 · 10^{15} cm) = 230 Schwarzschild radii r_s

X-ray: 0.34 ld = 21 r_S

$(r_s = 2GM_{grav}/c^2)$